Spiking dynamics of bidimensional integrate-and-fire neurons

Jonathan Touboul, Romain Brette

INSTITUT NATIONAL DE RECHERCHE EN INFORMATIQUE ET EN AUTOMATIQUE

Spiking dynamics of bidimensional integrate-and-fire neurons

Jonathan Touboul — Romain Brette

N° 6531

September 8, 2008

Thème BIO

ISSN 0249-6399 ISRN INRIA/RR--6531--FR+ENG

Spiking dynamics of bidimensional integrate-and-fire neurons

Jonathan Touboul * , Romain Brette

Thème BIO — Systèmes biologiques
Projet Odyssée †

Rapport de recherche n° 6531 — September 8, 2008 — 52 pages

Abstract: The class of non-linear integrate and fire neuron models introduced in the previous chapter, containing such models as the Izhikevich and the Brette-Gerstner ones, are hybrid dynamical systems defined both by a continuous dynamics, the subthreshold behavior, and a discrete dynamics, the spike and reset process. The dynamical properties of the subthreshold system has studied in [Touboul, 2008b]. This previous study does not account for the spiking properties of the model. We study in this chapter the spike patterns produced by these models. These patterns of activity are the result of an interplay between the continuous subthreshold dynamics and the reset process. Interestingly, the reset induces in bidimensional models behaviors only observed in higher dimensional continuous systems such as bursting and chaos.

This is why in the first section we study in depth the subthreshold dynamical system, and characterize its main dynamical properties, and a suitable framework in order to study the spike dynamics through the use of a discrete map, called the adaptation map. We then present how the spiking behavior of the model is linked with dynamical properties of the map, and show in particular that the system can exhibit a transition to chaos via period doubling, which was previously observed in Hodgkin-Huxley models and in Purkinje cells.

Key-words: No keywords

* jonathan.touboul@sophia.inria.fr
† Odyssée is a joint project between ENPC - ENS Ulm - INRIA

Unité de recherche INRIA Sophia Antipolis
2004, route des Lucioles, BP 93, 06902 Sophia Antipolis Cedex (France)
Téléphone : +33 4 92 38 77 77 — Télécopie : +33 4 92 38 77 65

Spiking dynamics of bidimensional integrate-and-fire neurons

Résumé : The class of non-linear integrate and fire neuron models introduced in the previous chapter, containing such models as the Izhikevich and the Brette-Gerstner ones, are hybrid dynamical systems defined both by a continuous dynamics, the subthreshold behavior, and a discrete dynamics, the spike and reset process. The dynamical properties of the subthreshold system has studied in [Touboul, 2008b]. This previous study does not account for the spiking properties of the model. We study in this chapter the spike patterns produced by these models. These patterns of activity are the result of an interplay between the continuous subthreshold dynamics and the reset process. Interestingly, the reset induces in bidimensional models behaviors only observed in higher dimensional continuous systems such as bursting and chaos.

This is why in the first section we study in depth the subthreshold dynamical system, and characterize its main dynamical properties, and a suitable framework in order to study the spike dynamics through the use of a discrete map, called the adaptation map. We then present how the spiking behavior of the model is linked with dynamical properties of the map, and show in particular that the system can exhibit a transition to chaos via period doubling, which was previously observed in Hodgkin-Huxley models and in Purkinje cells.

Mots-clés : Pas de motclef

1 Introduction

Recently in the neuro-computing community, finding a computationally simple and biologically realistic model of neuron has been a great endeavior. The main interest of this search is to get mathematically tractable models in order to understand the nature of the nerve cell activity, and computationaly simple in order to be able to compare experimental recordings with large scale brain models. The key problem is to find a model of neuron realizing a compromise between its simulation efficiency and its ability to reproduce what is observed at the cell level, often considering in-vitro experiments [Koch and Segev, 1998, Izhikevich, 2004, Rinzel and Ermentrout, 1989]. Among the variety of computational neuron models, nonlinear spiking models with adaptation have recently been studied by several authors [Izhikevich, 2004, Brette and Gerstner, 2005, Touboul, 2008b] and seem to stand out. They are relatively simple, i.e. mathematically tractable, efficiently implemented, and able to reproduce a large number of electrophysiological signatures such as bursting or regular spiking. These models feature the membrane potential of the nerve cell v togetger with an adaptation variable w, and distinguishes between to phases of the neuronal activity: the *subthreshold* behavior when no spike is emitted, and the emission of action potentials (spikes). The subthreshold dynamics is governed by the following ordinary differential equation:

$$\begin{cases} \frac{\mathrm{d}v}{\mathrm{d}t} = F(v) - w + I \\ \frac{\mathrm{d}w}{\mathrm{d}t} = a(bv - w) \end{cases} \tag{1.1}$$

where a, b are non-negative parameters accounting respectively for the time constant ratio between the adaptation variable and the membrane potential and b to the coupling strengh between these two variables. I is a real parameter accounting for the input current of the neuron, which in this mathematical study is assumed to be constant, and F is a real function accounting for the nonlinear ionic currents. Following [Touboul, 2008b], it is assumed to be regular (at least three times continuously differentiable), strictly convex, and its derivative to have a negative limit a $-\infty$ and an infinite limit at $+\infty$. In order to ensure that the neuron will elicit spikes, we add the following assumption:

Assumption (A1). *There exists $\varepsilon > 0$ such that F grows faster than $v^{1+\varepsilon}$ when $v \to \infty$ (i.e. there exists $\alpha > 0$ such that $F(v)/v^{1+\varepsilon} \geq \alpha$ when $v \to \infty$.*

We prove in section 2.5 that the membrane potential blows up in finite time in these cases. Among these models, the *quadratic adaptive* model [Izhikevich, 2004] corresponds to the case where $F(v) = v^2$, and has been recently used by Eugene Izhikevich and coworkers [Izhikevich and Edelman, 2008] in very large scale simulations of neural networks. The *adaptive exponential* model [Brette and Gerstner, 2005] corresponds to the case where $F(v) = e^v$ modeling the sodium current responsible for the generation of action potentials is modelled by an exponential function, following the work of [Fourcaud-Trocme et al., 2003], and has the interest that its parameters can be related to electrophysiological quantities, and has been successfully fit to intracellular recordings of pyramidal cells [Clopath et al., 2007, Jolivet et al., 2008]. The *quartic* model [Touboul, 2008b] corresponds to the case where

$F(v) = v^4 + 2a\,v$ and has the advantage to of being able to reproduce all the behaviors featured by the other two and also self-sustained subthreshold oscillations which are of particular interest to model certain nerve cells.

As we have seen in [Touboul, 2008c] and in section 2.5, in the case of the adaptive quadratic model or when the function F diverges slower than v^2 when $v \to \infty$ (i.e. when there exists $V_F > 0$ such that $F(v)/v^2$ is bounded for $v \geq V_F$), the adaptation variable blows up at the same time as the membrane potential. In these cases, a spike is emitted at the time t^* when the membrane potential v reaches a cutoff value θ. At this time, the membrane potential is reset to a constant value v_r and the adaptation variable is updated to $w(t^*) + d$ where $w(t^*)$ is the value of the adaptation variable at the time of the spike and $d > 0$ is the spike-triggered adaptation parameter. Because of the explosion of the adaptation variable, it is mandatory to define an arbitrary cutoff, as done in [Izhikevich, 2007]. The spiking properties are highly sensitive to changes in this cutoff parameter, as proved in [Touboul, 2008c].

For this reason, we will not be interested in this type of models, but will rater study models having intrinsic properties. This is why in the rest of the paper we consider models with an F function satisfy the following assumption:

Assumption (A2). *There exists $\varepsilon > 0$ such that F grows faster than $v^{2+\varepsilon}$ when $v \to \infty$ (i.e. there exists $\alpha > 0$ such that $F(v)/v^{2+\varepsilon} \geq \alpha$ when $v \to \infty$.*

In these cases as proved in [Touboul, 2008c] and in section 2.5, the membrane potential blows up in finite times and at these times the adaptation variable converges to a finite value. A spike is emitted at the time t^* when the membrane potential blows up. At this time, the adaptation variable converges to the value

$$w(t^*) \stackrel{\text{def}}{=} \left(\lim_{t \to t^*} w(t) \right).$$

After the spike emission, the membrane potential is reset to a constant value v_r and the adaptation variable is added a positive parameter, the spike-triggered adaptation parameter:

$$v(t) \text{ blows up at time } t^* \implies \begin{cases} v(t^*) & \leftarrow v_r \\ w(t^*) & \leftarrow w(t^*) + d \end{cases} \tag{1.2}$$

In these models, the reset mechanism makes critical the value of the adaptation variable at the time of the spike. Indeed, when a spike is emitted at time t^*, the new initial condition of the system (1.1) is $(v_r, w(t^*) + d)$. Therefore, this value governs the subsequent evolution of the membrane potential, and hence the spike pattern produced.

These models are *hybrid* dynamical systems, in the sense that they are defined by both a continuous and a discrete dynamical system. This structure make these models very interesting. Indeed the addition of the reset to the bidimensional continuous dynamical systems makes possible behaviors which cannot appear in autonomous bidimensional nonlinear ordinary differential equations, such as the bursting and chaos (see

[Izhikevich, 2003, Brette and Gerstner, 2005, Touboul, 2008a]). In this chapter we will rigorously study from a mathematical point of view these different behaviors, in order to understand qualitatively the origin of the different observed behaviors, and quantitatively to get insights on the ranges of parameters to obtain a given behavior.

To this end, we precisely study in section 2 the orbits of equation (1.1) in the phase plane (v, w) in order to characterize the value of the adaptation variable at the time of the spike. We will be particularly interested in the attraction basins of the stable subthreshold orbits. We will define herein an essential tools to study the spike patterns, the adaptation (or Poincaré) map. We observe that the properties of this map are closely linked with the subthreshold dynamics properties, more precisely with the number and stability of fixed points. Section 3 will be devoted to the case where the subthreshold system has no fixed point, and in the case where the neuron fires whatever its initial condition. Therefore the study of the iterations of the map Φ allows us to discriminate between different modes of tonic spiking. Section 4 is devoted to the case where there exist non-spiking subthreshold orbits. In these cases depending on the initial condition the system can either fire infinitely many spikes (tonic spiking) or finitely many spikes (phasic spiking). In the last section 5 we comment these results from a neurocomputational viewpoint.

2 Detailed study of the subthreshold dynamics

The class of systems we study here is the general class of nonlinear bidimensional neuron models introduced in [Touboul, 2008b]. We recall here briefly for the sake of completeness the main definitions. These models feature the neuron's membrane and an adaptation variable, whose coupled dynamics is the superpositions of two mechanisms: a nonlinear subthreshold integration mechanism, driven by the ordinary differential equation (1.1), coupled with the spike-and-reset mechanism given by equation (1.2). If membrane potential blows up at time t^*, a spike is fired, and subsequently the membrane potential is instantaneously reset to a constant value v_r and the adaptation variable is increased by a constant value d.

This system is an *hybrid dynamical system*: it is defined by both a continuous time dynamical system given by the equations (1.1) and a discrete dynamical system called the spike and reset mechanism, given by the equations (1.2), with five real parameters (a, b, I, v_r, d). The parameters (a, b, I) govern the subthreshold dynamics, while the parameters v_r and d govern the spike and reset mechanism. The subthreshold bifurcation problem was first studied by Izhikevich in [Izhikevich, 2006] in the case of the adaptive quadratic integrate and fire model, and extended to the generalized class of models of [Touboul, 2008b]. It appears that a is not a bifurcation parameter, and that the system undergoes a subcritical Bogdanov-Takens bifurcation. Moreover, under a simple condition on F and the other parameters, the model can undergo a Bautin bifurcation. This analysis accounts for the subthreshold behavior of the neuron and allows one to define *electrophysiological classes* of neurons depending on the parameters of the model, as done in [Touboul and Brette, 2008] in the case of the adaptive exponential model.

Nevertheless, this former study does not explain the spiking behaviors of the neuron, which are governed by the spiking mechanism. These properties are closely linked with topological properties of the underlying dynamical system, and we are interested here in understanding these properties. In this section, we first recall the main results of [Touboul, 2008b] on the subthreshold dynamics, which will be useful in the rest of the paper, and extend these results by studying the topological properties of the dynamical system defined by (1.1). We will see that there are three types of subthreshold orbits (i.e. orbits which will never fire): the ones that are attracted towards a stable fixed point of the dynamical system, the ones attracted by a limit cycle, and the stable manifold of the possible saddle fixed point. We will see that this stable manifold will shape the attraction basins of the stable subthreshold orbits (fixed points or limit cycles). This detailled study of the subthreshold dynamics will lead us to define a Markov partition of the dynamics, and will allow us to prove that that except from solutions of with initial condition on the stable manifold of the saddle fixed point or in the attraction basin of the stable subthreshold orbit, all the solutions fire a spike and are reset. We characterize the orbits of the solutions in the phase plane (v, w) and show conclude that the problem (1.1) together with (1.2) is well posed. Therefore, we will be able to study the spike patterns given any initial condition. To this end we lastly introduce the Poincaré application which will be essential in the study of the spike patterns.

2.1 Subthreshold bifurcations

Because of existence and uniqueness of solution obtained in proposition 2.3, we conclude that the whole dynamics between two spikes depends only on the initial condition of the neuron. The way the elicits a spike is mainly linked with the subthreshold dynamics, and define electrophysiological classes depending on the subthreshold dynamics parameters a, b and the input current I. This issue has been investigated in [Touboul, 2008a, Touboul and Brette, 2008]. We summarize here the results obtained. Let us denote $v^*(x)$ the unique solution, when it exists, of the equation $F'(v^*(x)) = x$. Let us denote by $F'_{-\infty}$ the limit of $F'(x)$ for $x \to -\infty$. This value can be either finite (but nonpositive) or equal to $-\infty$. Note that because of the strict convexity assumption, if there exists a solution, it is unique. Furthermore, solutions exist for any $x \in (F'_{-\infty}, \infty)$. Let us denote also $m(x) = F(v^*(x)) - xv^(x)$. It is the unique minimum, when $v^(x)$ exists, of $t \mapsto F(t) - x\,t$. We have:

Theorem 2.1. *The number and the stability of the fixed point of the subthreshold system depends on the parameters of the system in the following fashion:*

1. *If $I > -m(b)$, then the system has no fixed point.*
2. *If $I = -m(b)$, then the system has a unique fixed point, $(v^*(b), w^*(b))$, which is non-hyperbolic. It is unstable if $b > a$. Along this curve in the parameter space (I, b), the system undergoes a saddle-node bifurcation provided that $F''(v^*(b)) \neq 0$.*

3. *If $I < -m(b)$, then the dynamical system has two fixed points $(v_-(I,b), v_+(I,b))$ such that*
$$v_-(I,b) < v^*(b) < v_+(I,b).$$
The fixed point $v_+(I,b)$ is a saddle fixed point, and the stability of the fixed point $v_-(I,b)$ depends on I and on the sign of $(b-a)$:
   (a) *If $b < a$, the fixed point $v_-(I,b)$ is attractive.*
   (b) *If $b > a$, it depends on the input current I with respect to the value $I_H(a,b) = bv^*(a) - F(v^*(a))$.*
   (c) *At the point $b = a$ and $I = -m(a)$, the system undergoes a Bogdanov-Takens bifurcation provided that $F''(v_a) \neq 0$. Therefore, from this point, there is a saddle homoclinic bifurcation curve characterized in the neighborhood of the Bogdanov–Takens point by*
$$(P) := \left\{ (I, b \geq a)\ ; I_{Sh} = -m(a) + -\frac{12}{25}\frac{(b-a)^2}{F''(v^*(a))} + o(|\,(b-a)^2\,|) \right\}. \quad (2.1)$$
      i. *If $I < I_H(a,b)$, the fixed point $v_-(I,b)$ is attractive.*
      ii. *If $I > I_H(a,b)$, the fixed point $v_-(I,b)$ is repulsive.*
      iii. *On the parameter line given by*
$$(AH) := \left\{ (b, I)\ ;\ b > a \ \text{ and } \ I = bv^*(a) - F(v^*(a)) \right\},$$
the system undergoes an Andonov Hopf bifurcation, whose type is given by the sign of the variable
$$A(a,b) = F'''(v^*(a)) + \frac{1}{b-a}F''(v^(a))^2.$$
If $A(a,b) > 0$, then the bifurcation is subcritical, and if $A(a,b) < 0$, then the bifurcation is supercritical. If furthermore we have $F'''(v^*(a)) < 0$ and some technical conditions fulfilled, then the system undergoes a Bautin bifurcation at the point $v^*(a)$ for $b = a - \frac{F''(v^(a))^2}{F'''(v^*(a))}$ and $I = bv^*(a) - F(v^*(a))$.

To describe further the subthreshold dynamics we consider that the phase plane is either separated in three or five regions, depending on the existence of fixed points or not. The description of these regions and the dynamics of the system between these regions is given in figure Fig.1. Note that in the case of 1.A, a trajectory in the South region can either keep in the south region or quit this region to enter the center region. Similarly, in the North region, it can either go East or West. We will precise this diagram later on in section 2.3.

The results on local and global bifurcation given in theorem 2.1 imply the existance of families of cycles, which we study further in the next section.

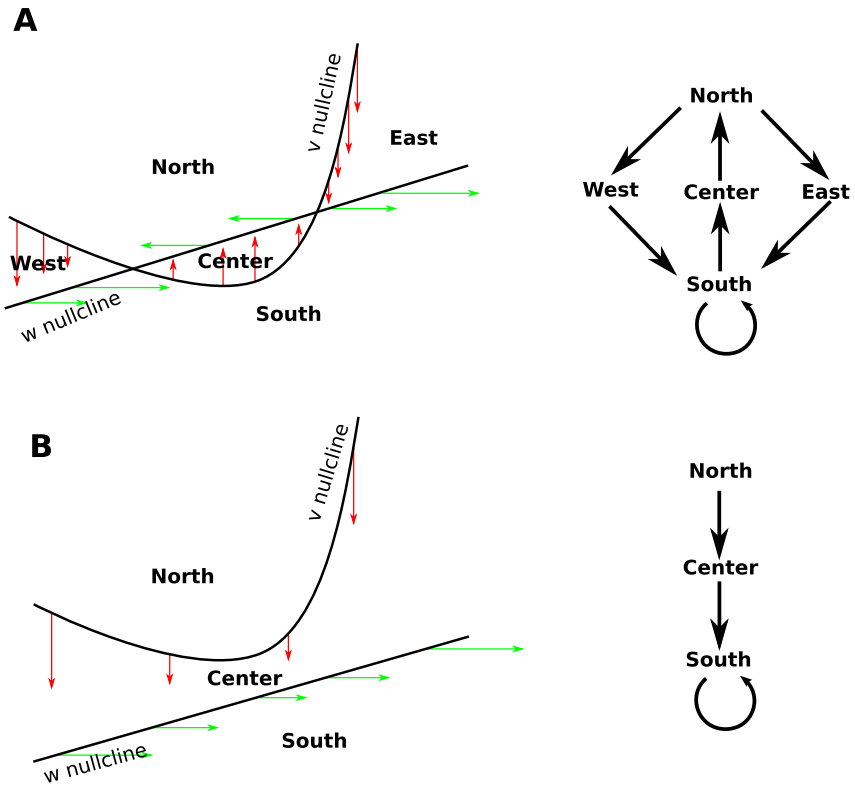

Figure 1: Nullclines of the dynamical system (horizontal axis: v; vertical axis: w). A. The nullclines intersect in two points, and divide the phase space into 5 regions. The potential V increases below the V-nullcline, w increases below the w-nullcline. The direction of the flow along each boundary gives the possible transitions between regions (right). Spiking can only occur in the South region. B. The nullclines do not intersect. All trajectories must enter the South region and spike.

2.2 Periodic orbits

In this section we characterize the number and the type of limit cycles of the system. The problem of determining the number and location of limit cycles for an autonomous planar vector field is a very complex problem for general dynamical systems, ans the case of a polynomial vector fields is still unresolved[1]. Nevertheless, for simple systems such as the one we are studying here, a complete description of the limit cycles is possible.

First of all, in the case $I > -m(b)$ (i.e. no fixed point for the subthreshold dynamics), it is clear that no limit cycle can exist, because of the shape of the vector field (see figure 1B.). Indeed, if a limit cycle exists, it will necessarily cross both nullcline, but any orbit entering the South region keeps trapped in this region. Hence no closed orbit exist in that case.

When decreasing the current, the system will undergo a saddle-node bifurcation, two fixed points will appear, but no cycle will be generated. Hence the system has no cycle for $b < a$.

For $b > a$, when decreasing further the input current, the system will undergo a Hopf bifurcation, which will generate a branch of limit cycles. These limit cycles are repulsive if the system does not undergo a Bautin bifurcation, and are attractive for $b > a - \frac{F''(v^(a))^2}{F'''(v^*(a))}$ if the system satsifies the conditions of the Bautin bifurcation. The saddle-node and Andronov-Hopf bifurcations collide via a Bogdanov-Takens bifurcation at the point $b = a$. In the neighborhood of this bifurcation, the family of limit cycles collide with the saddle fixed-point manifold and disappears via a saddle-homoclinic bifurcation. The saddle homoclinic bifurcations manifold can be written in the neighborhood of the Bogdanov-Takens bifurcation as a function $(b, I = I_{Sh}(a, b))$ having the quadratic expansion given by equation (2.1), and can be completely computed numerically using a continuation algorithm.

1. When the Hopf bifurcation is subcritical, the system presents a stable fixed point surrounded by a repulsive limit cycle for $I_H(a, b) < I < I_{Sh}(a, b)$, an homoclinic orbit for $I = I_{Sh}(a, b)$ and no limit cycle for $I > I_{Sh}(a, b)$.

2. When the Hopf bifurcation is supercritical, the system has an unstable fixed point surrounded by an attractive limit cycle for $-m(b) < I < I_H(a, b)$ and no cycle for $I < I_H$.

Let us decribe a little bit further the shape of these periodic orbit when it exist. Because of the structure of the shape of the vector field presented in figure 1.B., cycles necessarily include the fixed point v_-, and do not include the fixed point v_+, because the South zone intersected with the set $\{v \geq v_+\}$ is stable and no trajectory can escape from this zone. At a subcritical Hopf bifurcation, cycles appear around the fixed point v_-, and inflate when decreasing the input current until reaching the saddle fixed point v_+.

The presence of periodic orbits shape the structure of the stable manifold of the saddle-fixed point. We describe now the topology of this stable manifold and the shape of the attraction basins of the possible stable subthreshold orbits.

[1] it is the 16^{th} of the 23 problems of David Hilbert

2.3 Stable manifold and attraction basins

In this chapter we call *subthreshold orbit* any solution of the differential system (1.1) that do not fire, i.e. whose membrane potential does not blow in finite time. In the systems we study, subthreshold orbits can be of different type: fixed points, limit cycles, orbits converging to the stable fixed points or the stable periodic orbits, and the stable manifold of saddle fixed points.

We are interested in this section in the structure of the attraction basins of stable subthreshold orbits (SSO). A point (v, w) belongs to the attraction basin of a SSO if and only if the system (1.1) starting from this point converges towards this orbit. The topology of this set is governed by the subthreshold dynamics, and the problem of identifying in a closed form the attraction basin of the SSOs is very hard to handle formally. Nevertheless in our particular case we can describe the sets qualitatively. Indeed, when such a bounded stable trajectory exists, there always exists a saddle fixed point, and the structure of the attraction basin will be closely related to the structure of the stable manifold of the saddle fixed point (SMSFP).

The first order expansion of the SMSFP around the saddle fixed point is given by the eigenvalues and eigenvectors of the Jacobian matrix at this point. The SMSFP is composed of two submanifolds: one of them is locally contained in the zone $v \geq v_+$ which we denote Γ^+ and the other in the zone $v \leq v_+$, which we denote Γ^-. In all the cases, the submanifold Γ^+ is fully contained in the v-nullcline (i.e. $w \geq F(v) + I$), because of the direction of the eigenvectors of the Jacobian matrix at this point. This submanifold keeps in the Noth zone and this curve is the graph of an increasing function of v. The shape of the submanifold Γ^- locally satisfying $v \leq v_+$ depends on finner properties of the vector field, as we discuss in the sequell and in section 2.4.

First of all, in the case where $b > a$ and $I \in (I_{Sh}, I_H)$, there exists a repulsive periodic orbit circling anti-clockwise around the stable fixed point. First of all, since this orbit is a trajectory of the dynamical system, no solution can cross it because of Cauchy-Lipschitz theorem. The attraction basin of the stable fixed point will therefore be delineated by the periodic orbit: any trajectory having its initial condition inside this closed orbit will necesarily converge to the fixed point because of Poincaré-Bendixon's theorem, and no solution starting outside this zone can converge towards this fixed point because trajectories will not cross (Cauchy-Lipschitz' theorem). Therefore, the attraction basin of the stable fixed point is the zone in the phase plane delineated by the unstable limit cycle. In that case, the submanifold Γ^- winds around this cycle. Indeed, this submanifold can be computed using the backward equation related to (1.1). If it is an unbounded orbit, this stable manifold will split the phase plane into two zones, one of which containing the unstable limit cycle and the stable fixed point. Any trajectory starting in the zone containing the stable fixed point will either converge to the fixed point if it is inside the attraction basin of this fixed point delineated by the unstable periodic orbit, or will be trapped inside this zone and will not enter inside the periodic orbit. In the latter case, this trajectory cannot diverge because of the structure of the trajectories. Poincaré-Bendixon theorem would imply that there exists a stable fixed point or a stable periodic orbit in this zone which is not the case. Therefore

the shape Γ^- will necessarily be bounded, and because of Poincaré-Bendixon's theorem, it will either converge to a fixed point or to a periodic orbit. Since there is no stable fixed point reachable by the stable manifold (the stable fixed point is repulsive for the backwards dynamics), this orbit will converge to the limit cycle (see figure 2(a)).

In the cases where there is no unstable limit cycle around the SSO (i.e. for $b < a$, or $b > a$ and $I < I_{Sh}$ in the cases where the SSO is a fixed point, or in the case where the SSO is a periodic orbit), the attraction basin of the SSO will be unbounded, and its shape will be deduced from the shape of the SMSFP.

For the submanifold Γ^-, several cases can occur:

- The stable manifold of the saddle fixed point can cross both nullclines (see figure 2(b)). As proved in section B or in [Touboul and Brette, 2008], this will be the case when $F'_{-\infty} > -\infty$ and if $b \geq \frac{(F'_{-\infty}+a)^2}{4a}$,
- It can cross the w-nullcline (which will always be the case when $a < -F'_{-\infty}$) but not the v-nullcline. In this case, the SMSFP is the graph of a function of v, that will be decreasing before it crosses the nullcline and increasing after this point (see figure 2(d)),
- It can cross no nullcline, and in this case the separatrix is the graph of an increasing function of v (see figure 2(c)).

In these cases, the SMSFP is unbounded, and splits the phase plane into two connected components, one of which containing the SSO. This component is the attraction basin of the SSO, because of Poincaré-Bendixon and Cauchy Lipschitz theorems.

2.4 Heteroclinic orbits

In the case where there are two unstable fixed point, one of which is repulsive and the other saddle, then the component Γ^+ of the SMSFP has the same properties as in the case where there existed SSOs: it is the graph of an increasing function of v for $v \geq v_+$. The submanifold Γ^- will connect to the repulsive fixed point, for the same reasons as mentionned in the case of the presence of an unstable limit cycle. Indeed, if we consider the backward equation starting in the neighborhood of the saddle fixed point, the repulsive fixed point of the forward dynamics becomes attractive, and it is the unique bounded trajectory possible. The stable manifold when considering the backward equation will either converge to the fixed point, or will diverge, according to Poincaré-Bendixon's theorem. But assuming that it is unbounded leads to a contradiction: if it is unbounded, it separates two zones (see figure 2), one of which containing the unstable fixed point. A trajectory having its initial condition in this zone will be trapped in it for all $t > 0$. But in this zone, the trajectory will be bounded because of the structure of the vector field, but their is no fixed point nor stable periodic orbit. Therefore Poincaré-Bendixon's theorem leads to a contradiction, and the stable manifold necesarily connects to the repulsive fixed point. This connection can be one of two types (see figure 3: a monotonous connection in the case where the eigenvalues

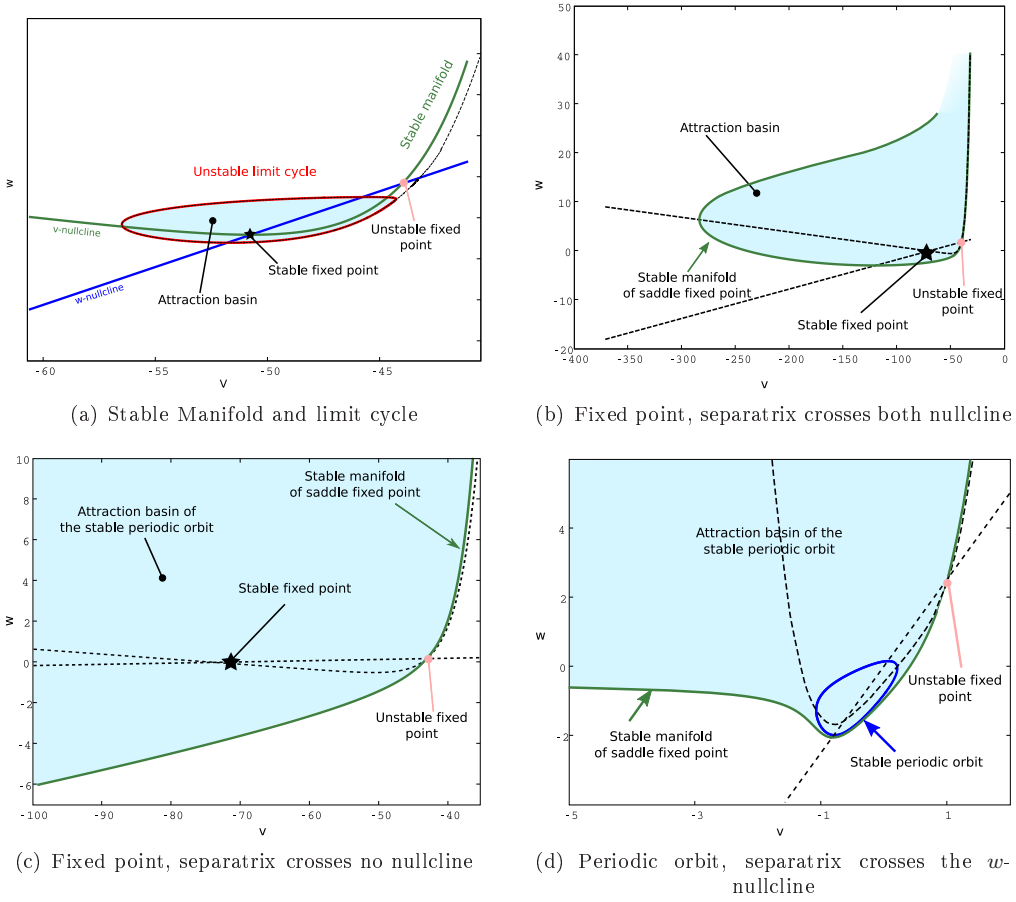

(a) Stable Manifold and limit cycle

(b) Fixed point, separatrix crosses both nullcline

(c) Fixed point, separatrix crosses no nullcline

(d) Periodic orbit, separatrix crosses the w-nullcline

Figure 2: Representation of the attraction basin and the stable manifold of the saddle fixed point in different cases. Figure 2(a) corresponds to the case where there exists a repulsive limit cycle around the stable fixed point. The red line corresponds to this fixed point, the back dased line to the stable manifold (see the indications in the figure). In the other three figures, we represented the case where there is no limit cycle in the phase plane. The dashed black line represent the nullclines, the green line the stable manifold of the saddle fixed point and the blue region the attraction basin of the stable trajectory. Figure 2(b) corresponds to the case where the separatrix crosses both nullclines: it returns in the direction $v > 0$ but will never reach the other part of the stable manifold (case of the AdExp model with original parameters but $a = 2g_L$ and $\tau_m = \tau_w$); 2(c) is the case where the stable manifold crosses no nullcline: it is the graph of an increasing function of v which delineates the attraction basin of the stable fixed point ((case of the dimensioned AdExp model with the original parameters but $a = 2g_L$ and $\tau_w = \tau_m/3$); 2(d) is the case where the stable manifold only crosses the w-nullcline. It was represented in the case where the stable trajectory is a periodic orbit (quartic model, $a = 1$, $b = 2.51$, $I = -0.5$).

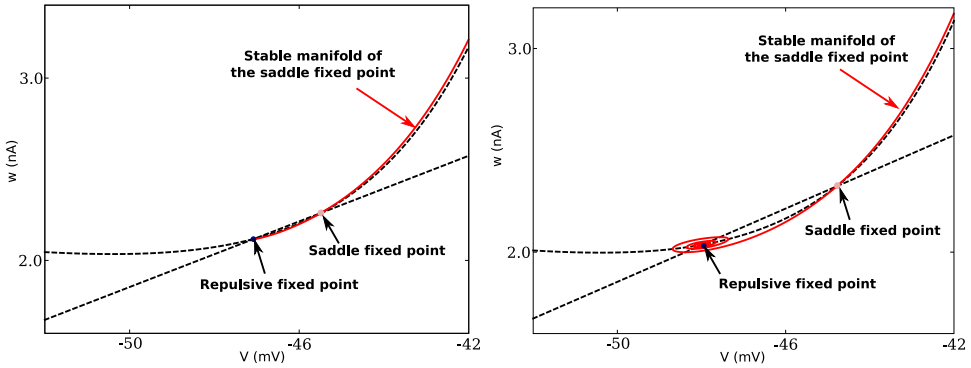

(a) Monotonous connection to equilibrium (b) Oscillatory connection to equilibrium

Figure 3: Stable manifold of the saddle fixed point in the case of two unstable equilibria. Dashed black curves are the nullclines of the system and the red curve is the stable manifold.

of the Jacobian matrix of the repulsive fixed point are real, and an oscillating connection when the eigenvalues have a non-nul imaginary part. This branch of stable manifold is therefore an heteroclinic orbit, connecting a repulsive equilibrium to a saddle equilibrium. It is structurally stable, and disappears at the Hopf bifurcation. In the case where the Hopf bifurcation is subcritical, the heteroclinic orbit connecting the repulsive fixed point and the saddle fixed point converts into an heteroclinic orbit connecting the saddle fixed point with the repulsive limit cycle and we are in the case of figure 2(a). In the case where the Hopf bifurcation is supercritical (after Bautin bifurcation) the heteroclinic orbit will simply disappears. By continuity it will be after the bifurcation of type 2(b).

2.5 Symbolic dynamics and spiking regions

This detailled description of the subthreshold dynamics allows us to get a better insight of the dynamics and to make diagram 1 more precise. Indeed, we are now able to provide a Markov partition of the phase plane.

- Where there is no fixed point (see fig.4(a)), we part the phase plane into the *up zone* above the v-nullcline, i.e. defined by $\{(v,w); w \geq F(v) + I\}$, the *center zone* between the two nullclines and the spiking zone below the w-nullcline $\{(v,w);\ w \leq b\,v\}$. We observe that any trajectory having its initial condition in the up zone enters in finite time the center zone. Indeed, while the orbit in the up zone, the derivative of the adaptatation variable is strictly inferior to $-d(F(v) + I, b\,v)$ the distance between the two nullclines. In the center zone, w is decreasing and v is increasing. Because of the vector field along the v-nullcine, we observe that the orbit cannot enter back the up zone. Since in this zone w is a decreasing function of v and the boundary $b\,v$ an

increasing function, it will enter in finite time the spiking zone. In this spiking zone defined by $w \leq b\,v$, the trajectory keeps trapped, and the membrane potential will blow up in finite time in this zone.

- In the case where there are stable subthreshold orbits, we reviewed the different shapes of the related attraction basins. These regions corresponds to what we will call the *rest* region, are stable under the dynamics, and do not communicate with the other zones(see figures 4(b), 4(c) and 4(d)). We define here again the spiking zone below both the w-nullcline and the SMSFP. This zone is also stable under the dynamics. The *right* zone is the zone above the w-nullcline and below the SMSFP. In this zone, for any initial condition below the v-nullcline, v is increasing and w decreasing. Therefore, the derivative of v increases, and the orbit will enter the spiking zone in finite time, since the orbit is a non-increasing function of v and the boundary is strictly increasing. If the initial condition is in the right zone below the SMSFP and above the v-nullcline, both v and w will be decreasing and therefore the orbit cannot stay above the v-nullcline indefinitely, because of the presence of the unstable manifold of the saddle fixed point, and therefore will be in the right zone below the v nullcline after a finite time, and therefore in the spiking zone in finite time. The *up* zone is the rest of the phase plane. In this zone, orbits do not stay indefinitely, and cannot enter neither the rest zone or the right zone, hence enter in finite time the spiking zone.

- In the cases where are two unstable fixed points and no stable limit cycles (Figures 4(e) and 4(f)), there is no stable subthreshold orbit (SSO) except from the SMSFP. We define the *up* zone above both the w-nullcline and the SMSFP, the right zone the zone between the SMSFP and the w-nullcline and the *spiking* zone below both the w-nullcline and the SMSFP. In the spiking zone, as we will see, the system will fire. For any initial condition in the right zone, since the orbit will not cross the SMSFP, it will necesarilly enter the spiking zone in finite time.

This is very important in terms of spikes. Indeed, we can prove that for any initial condition in the bottom region, the membrane potential v will blow up in finite time, and therefore a sike will be emitted. Indeed, let (v_0, w_0) be a given initial condition in the bottom region at time t_0. According to the shape of the vector field, as presented in our Markov partition, the whole trajectory will be trapped in this zone. But in this zone, we always have $w \leq v$ and therefore for all $t \geq t_0$ we have $w(t) \leq b\,v(t)$. According to Gronwall's theorem, the membrane potential at time $t \geq t_S$ will be greater or equall to the solution of:

$$\begin{cases} \dot{\tilde{v}} & = F(\tilde{v}) - b\,\tilde{v} + I \\ \tilde{v}(t_S) & = v(t_S) \end{cases}$$

which blows up in finite time by the virtue of assumption (A1).

Therefore any trajectory entering the bottom region will spike, and furthermore any trajectory having its initial condition outside the rest region will fall in the bottom region in finite time, and elicit a spike. As we have seen, the dynamics of the reset after a spike

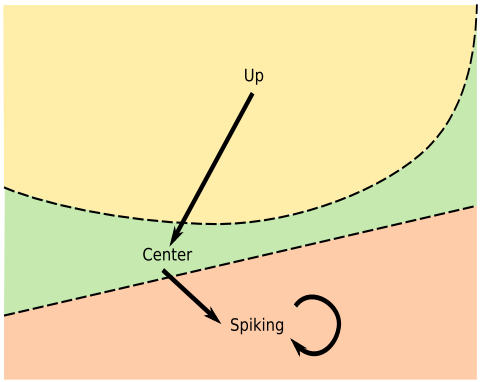

(a) No fixed point case

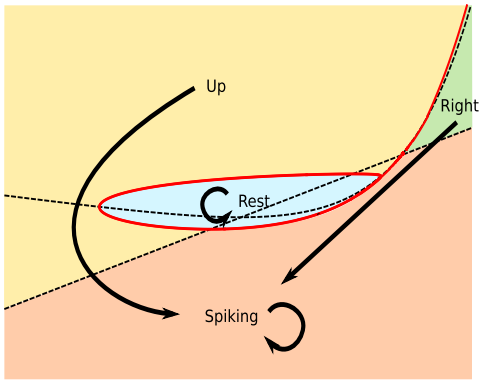

(b) Unstable limit cycle

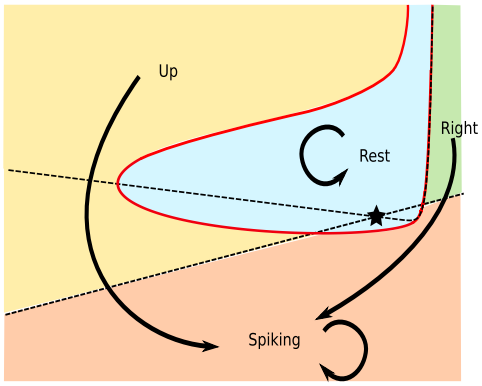

(c) Unbounded attraction bassin crossing both nullclines

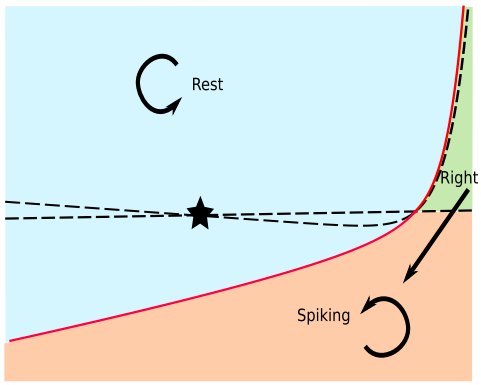

(d) Unbounded attraction bassin crossing no nullcline

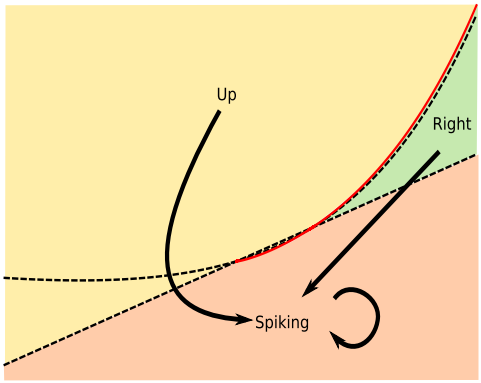

(e) Monotonous heteroclinic orbit

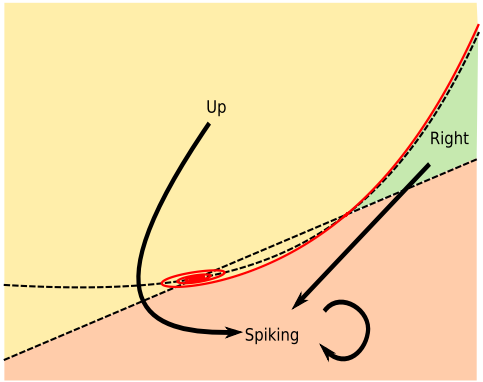

(f) Oscillatory heteroclinic orbit

Figure 4: Markov partition of the dynamics: the bottom region is a stable region where each trajectory starting from the up or right region will end up in finite time. The rest region composed of the attraction basin of the possible stable trajectory is an isolated region.

depends on the value of the adaptation variable at the times of the spikes, which we describe in the following section.

2.6 Behavior of the adaptation at the times of the spikes

In the spiking zone, we have seen that the membrane potential blew up in finite time. This zone does not intersect the v-nullcline. Therefore, in this zone, the orbit (v, w) with initial condition (v_0, w_0) at time t_0 inside the spiking zone can be written as the graph of a function of v for all $t \geq t_0$, i.e. $w(t) = W(v(t))$ where the function W is the solution of the differential equation:

$$\begin{cases} \frac{\mathrm{d}W}{\mathrm{d}v} = \frac{a\,(b\,v - w)}{F(v) - w + I} \\ W(v_0) = w_0 \end{cases} \tag{2.2}$$

Proof. Let $\delta(t) = W(v(t)) - w(t)$. We have $\delta(t_0) = 0$ and furthermore, since the value of $F(v) - w + I > 0$, $\frac{\mathrm{d}\delta}{\mathrm{d}t} = \frac{\mathrm{d}W}{\mathrm{d}v}\frac{\mathrm{d}v}{\mathrm{d}t} - \frac{\mathrm{d}w}{\mathrm{d}t} = 0$, and hence $\delta(t) \equiv 0$. □

To study the value of the adaptation variable at the explosion time of the membrane potential, we simply study the limit of the equation of the orbits when $v \to infty$. We prove here that this value is finite under assumption (A2), and that if $F(v)/v^2$ is asymptotically bounded, the adaptation value tends to infinity. This theorem justifies the introduction of this assumption.

Theorem 2.2. *Under assumption (A2), the adaptation variable is finite at the times of the spikes. If $F(v)/v^2$ is bounded when $v \to \infty$, the adaptation variable at the times of the spikes tends to infinity.*

Proof. In section 2.5, we proved that all the orbits of the system that are not in the attraction basin of the possible stable fixed point will be trapped after a finite time the *spiking zone* fully included in the half space $\{w < b\,v\}$ and in this zone the membrane potential blows up in finite time.

The value of the adaptation variable at the time of the spike can therefore be computed using the orbital equation (2.2). We consider $(v(t), w(t))$ an orbit of the differential system (1.1) such that the membrane potential blows up at time t^*. Let $(v_1 = v(t_1), w_1 = w(t_1))$ a point of the orbit inside the spiking zone. We recall that In the spiking zone, we have $w(t)) \leq b\,v(t)$ and $w(t)$ is non-decreasing. Hence we have

$$\frac{\mathrm{d}W}{\mathrm{d}v} \leq \frac{a\,(b\,v - w_1)}{F(v) - b\,v + I} \tag{2.3}$$

and hence

$$W(v) \leq \int_{v_1}^{v} \frac{a\,(b\,u - w_1)}{F(u) - b\,u + I}\,du$$

If F satisfies assumption (A2), then the this integral converges when $v \to \infty$. Therefore, $W(v)$ (resp. $w(t)$) is an upperbounded nondecreasing function of v (resp. time), and therefore has a finite value when $v \to \infty$ (resp. $t \to t^*$).

In the case where $F(v)/v^2$ is bounded, this integral does not converge. Let us lowerbound this value. Using the same technique, we have:

$$\frac{\mathrm{d}W}{\mathrm{d}v} \geq \frac{a\,(b-W)}{F(v)-w_1+I}. \tag{2.4}$$

Gronwall's theorem [Gronwall, 1919] ensures us that the solution of equation (2.2) will be lowerbounded for $v \geq v_1$ by the solution of the linear ordinary differential equation:

$$\begin{cases} \frac{\mathrm{d}z}{\mathrm{d}v} = \frac{a\,(b-z)}{F(v)-w_1+I} \\ z(v_1) = w_1 \end{cases} \tag{2.5}$$

that reads:

$$z(v) = \left(\int_{v_1}^{v} \frac{a\,b\,u}{F(u)-w_1+I} e^{-g(u)}\,du + w_1) \right) e^{g(v)}$$

where $g(v) = \int_{v_1}^{v} -\frac{a\,du}{F(u)-w_1+I}$. Because of assumption (A1), the integrand is integrable, and the function g has a finite limit $g(\infty)$ when $v \to \infty$. The exponential terms will hence converge when $v \to \infty$. But the integral involved in the particular solution diverges in the case where $F(v)$ grows slower than v^2, since the integrand is equivalent when $u \to \infty$ to

$$\frac{a\,b\,u}{F(u)} e^{-g(\infty)}$$

When $F(u)$ grows slower than v^2 there exists $\alpha > 0$ such that $F(v) \leq \alpha v^2$ asymptotically and therefore the solution of the linear differential equation (2.5) tends to infinity when $v \to \infty$ faster than a logarithmic function of v, and so does $W(v)$, and hence $w(t)$ blows up at the time when $v(t)$ blows up. In the case where $F(v)$ grows slower than $v^{2-\varepsilon}$, the solution of the differential equation diverges faster than v^{ε}. □

We therefore conclude that in the case of the quadratic adaptive model, the adaptation variable blows up at the explosion time of the membrane potential variable v, and in the case of the quartic and exponential models, the adaptation variable remains bounded.

For the quadratic models, and models such that the nonlinear function $F(v)$ grows slower than a quadratic function when $v \to \infty$, the system can only be defined using a cutoff value for the spikes. The value of the adaptation variable at the cutoff θ will be given by $W(\theta)$, and therefore will heavily depend on the cutoff value.

In the quartic and exponential models, and for any model such that $F(v)$ grows faster than $v^{2+\varepsilon}$ for a given $\varepsilon > 0$, the adaptation variable converges, and hence the model can be defined with an infinite threshold. These models have intrinsic properties independently of the possible cutoff. As stated in [Touboul, 2008b], this property is very important to shape the spike patterns, and therefore we will be interested in this chapter only to models such that the adaptation variable converges. This is the reason why we introduce assumption (A2).

In these cases, for technical reasons we will use a transformed version of the orbital equation (2.2) obtained by changing variables. We consider $u = (v - v_0 + 1)^{-\varepsilon/2}$ where $\varepsilon > 0$ is given by assumption (A2). When $v(t)$ blows up, $u(t)$ tends to zero, and the orbit in the plane (v, u) satisfies the equation:

$$\begin{cases} \frac{\mathrm{d}\tilde{W}}{\mathrm{d}u} = -\frac{2a(bu^{-2/\varepsilon} - \tilde{W} + \beta)}{\varepsilon u^{1+2/\varepsilon}(F(u^{-2/\varepsilon} + v_0 - 1) - \tilde{W} + I)} =: g(u, \tilde{W}) \\ \tilde{W}(1) = w_0 \end{cases} \tag{2.6}$$

where $\beta = b\,(v_0 - 1)$

As we can see in equation (1.1), at the times where the membrane potential blow up and since the adaptation variable remains bounded, the derivative of adaptation variable tends to infinity when v blows up. For this reason, accurate numerical simulations are quite hard to perform. But in the phase plane, the orbit has a regular equation. Therefore, an accurate algorithm can be deduced from these facts. As soon as the orbit enters the spiking zone, one could simulate the orbital equation (2.2) in order to get a precise evaluation of the adaptation value at the time of the spike. Since the equation is regular, standard simulation algorithms can be used (Runge-Kutta, Euler, ...).

2.7 Existence and uniqueness of solution

We first discuss the well-posedness of these equations. Mathematically, the problem is well-posed if the system defined by equations (1.1) and (1.2) together with an initial condition (v_0, w_0) at time t_0 has a unique solution defined for all $t \geq t_0$. The precise study we just performed gives us a better understanding of the dynamics of the subthreshold system. In particular, we have seen that the solutions of the subthreshold equation (1.1) blew up in finite time, and under assumption (A2), the adaptation variable at these times has a finite value. The solutions of the subthreshold are hence not well defined for all time. The reset condition is therefore essential to have a forward solution to the problem defined for all $t \geq t_0$. The reset condition is sufficient for the problem to be well posed, as we prove in the following:

Proposition 2.3. The equations (1.1) and (1.2), together with initial conditions (v_0, w_0) at time t_0 has a unique solution defined for $t \geq t_0$.

Proof. Because of the regularity assumption on F, Cauchy-Lipschitz theorem of existence and uniqueness of solution applies for equation (1.1) up to the explosion time. If the solution of (1.1) do not blow up in finite time, we have therefore existence and uniqueness of solutions for the problem. If the solution blows up at time t^*, then we are reset to a unique point, defined by the reset condition 1.2, and we are again in the case we already treated starting from $(v_r, w(t^*) + d)$ at time t^*. We can apply this mechanism again provided since the value of $w(t^*)$ is finite. Furthermore, to be able to prove the existence and uniqueness of solution for all $t \geq t_0$, we need to ensure that the spike time does not tend to 0 (i.e. spikes do not accumulate at a given time location). The spike time decreases when the value of

the adaptation on the reset line decreases. Therefore we have to ensure that the adaptation value at the times of the spike do not tend to $-\infty$. But for w_0 in the spiking zone, the value of the adaptation variable is increasing all along the trajectory and therefore the new adaptation value after a spike is emitted will be greater than the former value plus d, and hence it is impossible that this reset value tends to $-\infty$. Therefore, the spike times have a lower bound on this trajectory, and between two spike times, we can prove a property of existence and uniqueness of solution. Therefore we have existence and uniqueness of a solution starting from (v_0, w_0) which is defined for any $t \geq t_0$. □

In this proposition, we proved that there existed a unique forward solution to the problem for a given initial condition.

Another interesting question would be to solve the related Cauchy problem. This problem consists in proving that there exists a unique solution defined for all $t \in \mathbb{R}$. The Cauchy problem problem was adressed by Romain Brette in [Brette, 2007] in the case of spiking models defined by a one dimensional ODE with a finite spiking threshold and a reset condition. He found that the reset introduced a countable and ordered set of backward solutions for a given initial condition, and this that this structure of solutions had important implications in terms of neural coding. The case of the system given by (1.1) and (1.2) can be treated in the same fashion as done in [Brette, 2007]. It is done in appendix A.

2.8 The Poincaré application

Now that we are ensured that there exists a unique solution to the forward problem given by equations (1.1) and (1.2), we are interested in characterizing the spike patterns fired by a neuron of this type. These patterns are governed by the initial condition of the system after each spike, and this is why we now introduce an essential element of our work, a discrete map called the Poincaré (or adaptation map).

Definition 2.1 (The adaptation (Poincaré) map)**.** We denote by $\mathcal{D}$ the domain of adaptation values w_0 such that the solution of (1.1) with initial condition (v_r, w_0) blows up in finite time. Let $w_0 \in \mathcal{D}$, and denote $(v(t), w(t))$ the solution of (1.1) with initial condition (v_r, w_0) and t^* the blowing time of v. The Poincaré map Φ is the unique function such that

$$\Phi(w_0) = w(t^*) + d$$

The Poincaré map gives the next reset location of a spiking orbit with initial condition on the *reset line* $v = v_r$. If we are interested in the spike patterns generated from an initial condition (v_0, w_0) where $v_0 \neq v_r$, the analysis will be valid after the first spike is emitted. More precisely, either (v_0, w_0) is in the attraction basin of a bounded trajectory or on the stable manifold of the saddle fixed point, then it will not elicit a spike. If it is not, then it will fire in finite time and be reset on the line $v = v_r$ at a given level, say w_1. From this point, the study of the iterations of the map Φ will be valid.

Moreover, assume that in the dynamical system defined by (1.1) starting from the initial condition (v_r, w_0) is in a tonic spiking behavior (i.e. fires after any given time T, hence

elicits infinitely many spikes). Then let $(t_n)_{n\geq 0}$ be the sequence of spike times, and define the sequence of adaptation reset points by $w_n := w(t_n) = w(t_n^-) + d$. The Poincare map of this dynamical system is the function Φ such that

$$\Phi(w_n) = w_{n+1}$$

Hence we will be able to apply techniques of nonlinear analysis of iterations of maps to study the spiking location sequences and the spiking times.

For these reasons, we will be interested in the sequel in the dynamics of the iteration of the map Φ which corresponds to a trajectory starting from an initial condition on the reset line. The intersections of the nullclines with the reset lines are of particular interest in the study of Φ. We omit for the sake of simplicity the dependency of these points with respect to the parameters, and define:

$$\begin{cases} w^* &= F(v_r) + I \\ w^{**} &= bv_r \end{cases} \tag{2.7}$$

Both point depend on the reset voltage v_r. Interestingly enough, besides v_r, the point w^* only depends on the input current and the nonlinearity, while the point w^{**} only depends on the parameter b. The figure Fig.5 represents bundles of trajectories for $w < w^*$ or $w > w^{**}$ in the case where the nullclines do not intersect. It illustrates the qualitative distinctions linked with the relative location of w with respect to w^*.

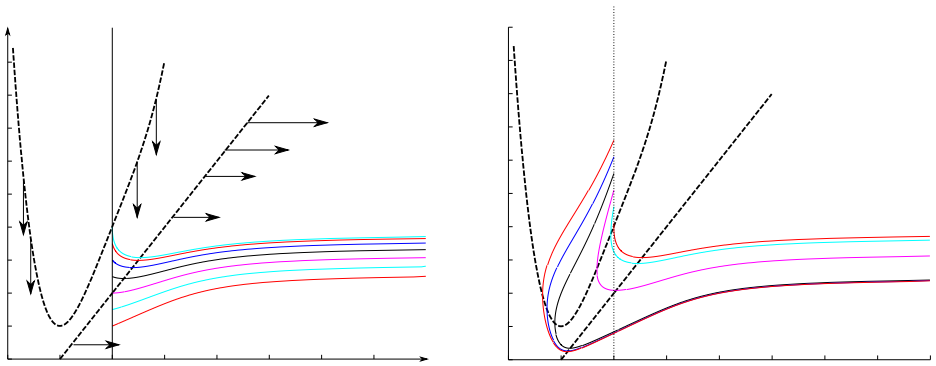

(a) Phase plane for $w_0 < w^*$ (b) Phase plane for $w_0 > w^*$

Figure 5: Phase plane and trajectories for the quartic model in the no-fixed point case. The trajectories starting from $w < w^{**}$ have an increasing w all along the trajectory, which is not the case for $w > w^{**}$. For $w > w^*$, we observe that the trajectory turns around the point (v_r, w^*) and crosses again the line $v = v_r$ before spiking.

The time it takes the neuron to elicit a spike governs the inter-spike interval. It is therefore a very pertinent information for a quantitative analysis of the models, or for

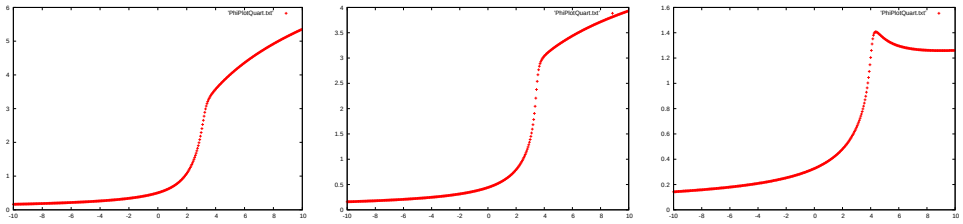

Figure 6: Spike times $\mathcal{T}$ function for the quartic model for different values of a and b. We can see that the function is not always increasing.

understanding the neural code. This map, as the Poincaré application Φ, is defined on the spiking domain $\mathcal{D}$ by: $\mathcal{T} : w \mapsto t^*(w)$ where $t^*(w)$ is the spike time if the membrane potential starts at (v_r, w) at time $t = 0$. If this map is one-to-one, then the reset location is directly linked with the interspike interval. Figure Fig.6 represents the map $\mathcal{T}$ in the case of the quartic model for different sets of parameters. We observe that this map is not always injective. Let us describe quickly its dynamics in the case where there is no fixed point for the subthreshold dynamics. In this case, $\mathcal{T}$ is defined for all $w \in \mathbb{R}$, it is increasing for $w \leq w^*$, as a straightforward application of the monotony of the modulus of the vector field with respect to w and the shape of the phase diagram partition in trajectories. For $w > w^*$, the trajectory turns around the point (v_r, w^*) and crosses again the curve $v = v_r$. Here again, it is clear that the time it takes for crossing again the curve $v = v_r$ increases with w. This time increase is compensated by the fact that when w increases, the second crossing location of the curve $v = v_r$ decreases. Eventually, as we prove in the sequel, the second crossing location of the curve $v = v_r$ has a lower bound, and hence after a given time, the map $\mathcal{T}$ will increases again.

As we will see, the non-injectivity of this map is not a big deal, and since we are interested in qualitative properties of the spiking, this map will not be of great interest in our study.

Now that we introduced the main framework of our study, we will study the main properties of this map. The different spike patterns are linked with the topology of the domain $\mathcal{D}$ and with properties of the map Φ. We chose here to present our results in function of the subthreshold dynamical properties, since it will make our mathematical analysis clearer. We will summarize the different regions of parameters for which a given spike pattern is produced in section 5.5.

3 No fixed point case

In this section we consider the case where there is no fixed point in for the subthreshold dynamical system. This case corresponds to the case where $I > -m(b)$ according to theorem 2.1. In that case the system has neither stable fixed point nor limit cycle, and hence no

bounded trajectory. The neuron will emit a spike whatever its initial condition. Indeed, let (v_0, w_0) be a given initial condition at time t_0 for the subthreshold system. According to the diagram 1, the trajectory will always be after a given finite time in the South zone, which corresponds in this case to the bottom zone. As already discussed in section 2.5, as soon as the trajectory enters this zone, it keeps trapped in this zone and blows up in finite time according to Gronwall's theorem.

Therefore, the definition domain of the Poincaré map is $\mathcal{D} = \mathbb{R}$: for any initial condition, the neuron will elicit a spike.

3.1 Description of the Poincaré application

We are now able to prove the following theorem.

Theorem 3.1. *In the case $I > -m(b)$ and under the condition (A2), the Poincaré map satisfies the following properties (see figure Fig.7):*

- *It is increasing on $(-\infty, w^*]$ and decreasing on $[w^*, \infty)$,*
- *For all $w < w^{**}$ then $\Phi(w) \geq w + d > w$,*
- *The map Φ is regular,*
- *It is concave for $w < w^*$,*
- *It has a unique fixed point in $\mathbb{R}$,*
- *It has an horizontal asymptote (plateau) when $w \to \infty$*

This theorem is quite important to understand the main properties of the *Poincaré sequence* w_n starting from a given initial condition $w_0 \in \mathcal{D}$ defined by:

$$w_{n+1} = \Phi(w_n) \tag{3.1}$$

These properties are straightforwardly proved if we had a spiking threshold, the only technical intricacy is the fact that the spike occurs when the membrane potential blows up.

Proof. The proof of this theorem is mainly based on a characterization of the orbits in the phase plane, given by equations (2.2) and (2.6). We have using these equations the orbits of the system starting initial condition (v_r, w_0) such that $w_0 \leq b\, v_r$:

$$\tilde{W}(u; w_0) = w_0 - \int_u^1 g(u, \tilde{W}(u, w_0))\, du. \tag{3.2}$$

We have in particular $\Phi(w_0) = \lim_{u \to 0} \tilde{W}(u, w_0)$.

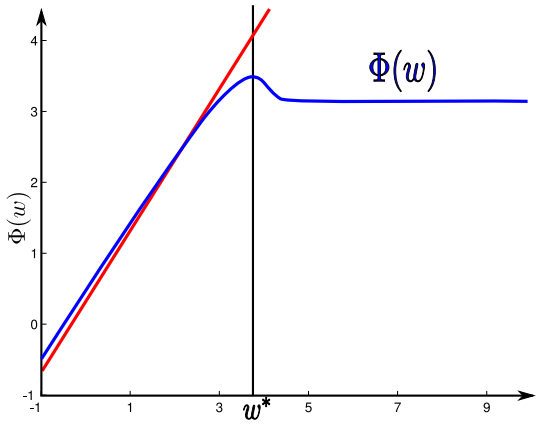

Figure 7: The Poincaré application Φ in the case of the quartic model for $I > -m(b)$ (no-fixed point). The blue line corresponds to the map Φ, the red line to the identity map and the black line localizes w^*. We can observe easily on this diagram the main properties of Φ in this case stated in theorem 3.1.

- *Monotony:* Let $w_1(0) < w_2(0) \leq w^*$. The orbits $(v_1(t), w_1(t))$ having initial condition $(v_r, w_1(0))$ at time $t = 0$ and $(v_2(t), w_2(t))$ having initial condition $(v_r, w_2(0))$ at time $t = 0$ will never cross because of Cauchy-Lipschitz theorem. Since they both are in the center or in the spiking zone of diagram 4(a), they satisfy equation (2.2) and therefore since they do not cross, we will always have $\tilde{W}_1(v) \leq \tilde{W}_2(v)$, and therefore $\Phi(w_1(0)) \leq \Phi(w_2(0))$.

  Let now $w^* \leq w_1(0) < w_2(0)$. In that case, the initial condition is in the up zone of diagramm 4(a). In this zone, we have seen that both variables v and w decrease in the up zone. The orbit enters in finite time in the center zone where v increases and w keeps decreasing. The orbits will therefore cross one time the reset line before spiking. This reset line is a Jordan section, and Jordan's theorem (see for instance [Dieudonné, 1963, Chap. 9, appendix, p. 246]) implies that the solutions are always ordered on this section, and the order of the adaptation value at the two new crossing positions w_1^1 and w_2^1 is inverted, i.e. $w_2^1 < w_1^1$. By application of the previous case, we obtain

  $$\Phi(w_1(0)) = \Phi(w_1^1) \geq \Phi(w_2^1) = \Phi(w_2(0)).$$

  We conclude that the map Φ is increasing on $(-\infty, w^*]$ and decreasing on $[w^*, \infty)$.

- *Behavior for $w < w^{**}$:* If $w < w^{**}$, then w will increase all along the trajectory, and hence $w(t_s) \geq w$ and hence $\Phi(w) \geq w + d$.

- *Regularity:* The regularity of Φ for $w < w^*$ comes from the theorem of regularity of the solution of an ordinary differential equation with respect to its initial condition. Since in the region $w < w^*$ (center and spiking regions of diagram 4(a)) the value of $F(v) - w + I$ never vanishes, the orbit starting from the initial condition (v_r, w_0) satisfy equations (2.2) in the plane (v, w) and equation (2.6) in the plane (u, w). In order to apply the regularity theorem with respect to the initial condition, we consider here equation (2.6) and check the regularity conditions.

  The function g is C^∞ in its variables on $(0, 1] \times \mathbb{R}$. We prove that it is regular at the point $u = 0$. First, the map g tends to 0 when $u \to 0$ because of condition (A2), since it is equivalent when $u \to 0$ to $-2ab/(\varepsilon u^{1+4/\varepsilon} F(u^{-2/\varepsilon} + v_r - 1))$ which tends to 0 ($F(u^{-2/\varepsilon} + v_r - 1) \leq \alpha u^{-4/\varepsilon - 2}$). Furthermore it is Lipschitz on $[0, 1]$ in the variable W since the partial derivative of this function reads:

$$\frac{\partial g}{\partial W} = \frac{2a}{\varepsilon u^{1+2/\varepsilon}} \frac{(F(u^{-2/\varepsilon} + v_r - 1) - b\,(u^{-2/\varepsilon} + v_r - 1) + I)}{(F(u^{-2/\varepsilon} + v_r - 1) - W + I)^2}$$

  This derivative is therefore positive, and because of the divergence of F and is equivalent when $u \to 0$ to $\varepsilon a/(2u^{1+2/\varepsilon} F(u^{-2/\varepsilon} + v_r - 1))$ which tends to zero because of assumption (A2). Therefore, using the theorem of Cauchy-Lipschitz with parameters, we conlude that the map $\tilde{W}$ is continuous with respect to the initial condition.

  But we can get even more regularity, provided that we prove that the map g has limits for its partial derivatives of higher order. The higher order partial derivatives of g with respect to W will converge to zero using the same argument, and by induction, we can prove that this is true for all the derivatives at 0 with respect to the variable W. The partial derivative with respect to u are slightly more intricate in the general case, but in the case of the quartic and exponential model, we can readily prove that this function g is C^∞ in (u, w) and therefore the theorem of Cauchy-Lipschitz with parameters implies that the map $W_\infty(\cdot)$ is C^∞.

  For $w \geq w^*$, the orbit will turn around the point (v_r, w^*). Hence Φ is the composition of the application giving the first crossing location of the orbit with the curve $\{v = v_r\}$ and Φ for $w < w^*$. The second is continuous because of the latter argument, and the first one is C^∞ because of the standard theory of Poincaré applications (theorem of Cauchy-Lipschitz with parameters for the system 1.1).

- *Concavity:* As already stated, for $w < w^*$, the solution of equation (1.1) will never cross the v nullcline, and the equation of the orbits in the phase plane (u, w) is given by equation 2.6, and the equation of the orbit given by equation (3.2). We have:

$$\begin{cases} \frac{\partial g}{\partial w} & = \frac{2a}{\varepsilon u^{1+2/\varepsilon}} \frac{F(u^{-2/\varepsilon}+v_r-1)-b\,(u^{-2/\varepsilon}+v_r-1)+I}{(F(u^{-2/\varepsilon}+v_r-1)-W+I)^2} > 0 \\ \frac{\partial^2 g}{\partial w^2} & = \frac{4\,a\,b}{\varepsilon u^{1+2/\varepsilon}} \frac{F(u^{-2/\varepsilon}+v_r-1)-b\,(u^{-2/\varepsilon}+v_r-1)+I}{(F(u^{-2/\varepsilon}+v_r-1)-W+I)^3} > 0 \end{cases} \tag{3.3}$$

  using the fact that $F(v) - w + I > 0$ and $w < b\,v$. Hence we have the following formula for the second derivative of φ with respect to w_0.

$$\frac{\partial^2 \tilde{W}}{\partial w_0^2} = -\int_u^1 \frac{\partial^2 g}{\partial \tilde{W}^2} \left(\frac{\partial \tilde{W}}{\partial w_0}\right)^2 + \frac{\partial g}{\partial \tilde{W}} \frac{\partial^2 \tilde{W}}{\partial w_0^2},$$

Because of inequalities (3.3) we have $\frac{\partial^2 \tilde{W}}{\partial w_0^2} \leq -\int_u^1 \frac{\partial g}{\partial \tilde{W}} \frac{\partial^2 \tilde{W}}{\partial w_0^2}$, and furthermore $\frac{\partial^2 \tilde{W}}{\partial w_0^2}(1, w_0) = 0$. Thus using Gronwall's theorem we obtain the convexity of the function $\tilde{W}(u, \cdot)$ for all u.

The Poincaré application Φ is defined by

$$\Phi(\cdot) = \lim_{u \to 0} \tilde{W}(u, \cdot)$$

Since g is at least C^2 in the second variable, so is the flow (Cauchy-Lipschitz theorem with parameters) and hence Φ has the same convexity property for $w < w^*$.

- *Existence and uniqueness of fixed point:* Let $w_0 < w^*$. Since we have for all $x < w^{**}$ the property: $\Phi(x) \geq x + d$ and for $x > w^*$, $\Phi(x)$ is a non-increasing function, we have existence of at least one fixed point. The uniqueness is given by the concavity of Φ for $w < w^*$ and the decreasing behavior of Φ for $w > w^*$.

- *Horizontal asymptote (plateau) :* The principle of the proof is to show that there exists a solution diverging to $-\infty$ when $t \to -\infty$. This solution will therefore cut the phase plane into two subdomains, and the orbits will be trapped in one or the other domain. In the zone above this solution, the map Φ will by decreasing and lowerbounded, hence will converge.

  To prove the existence of such a solution, we search for an invariant subspace of the phase plane for the backwards dynamics (i.e for the dynamical system $(v_b(t) = v(-t), w_b(t) = w(-t))$ which does not cross the v-nullcline $\mathbb{N} := \{w = F(v) + I\}$. We first search for solutions fully contained in a domain $\mathcal{B}$ bounded by two lines:

$$\mathcal{B} := \{(v, w) \mid v \leq v_0, w \leq w_0 + \alpha(v - v_0)\}$$

  We show that we can find real parameters (v_0, w_0, α) such that this domain is invariant by the dynamics and does not cross $\mathcal{N}$.

  First of all, for the boundary $\{v = v_0, w \leq w_0\}$, we want $\frac{\mathrm{d}v_b}{\mathrm{d}t} \leq 0$, which only means $w_b \leq w^*(v_0) = F(v_0) + I$.

  Now we have to characterize both v_0 , w_0 and α such that the vector field is flowing out of this affine boundary. This simply means that $\langle \binom{\dot{v}}{\dot{w}} | \binom{\alpha}{-1} \rangle \leq 0$ where $\langle \cdot | \cdot \rangle$ denotes the euclidian dot product. This condition simply reads $\alpha\dot{v} - \dot{w} \leq 0$ and has to be fulfilled on each point of the boundary, which is equivalent to:

$$a\Big(bv - w_0 - \alpha(v - v_0)\Big) \geq \alpha(F(v) - w_0 - \alpha(v - v_0) + I) \tag{3.4}$$

Using the assumption $\lim_{v\to-\infty} F'(v) < 0$, hence there exists an affine function such that for all $v \in \mathbb{R}$ $F(v) + I \geq uv + \beta$.

We consider now $\alpha < 0$. Then condition (3.4) implies that

$$\Big(ab - \alpha(u-\alpha) - a\alpha\Big)v + \Big(- aw_0 + \alpha a v_0 + \alpha w_0 - \alpha^2 v_0\Big) \geq 0$$

Hence the only thing to ensure is that $\Big(ab - \alpha(u-\alpha) - a\alpha\Big) < 0$. This condition is achieved when the discriminant of this equation is strictly positive, i.e. for all $u > 2\sqrt{ab} - a$ or $u < -2\sqrt{ab} - a$.

The initial condition on u was to be greater than the minimum of F', hence any $u > \max\big(2\sqrt{ab} - a, \min_{v\in\mathbb{R}} F'(v)\big)$ will be convenient.

In this case, for all $v < v_m$ and $w_0 < w_u$ the intersection of $\{v = v_m\}$ and the tangent at F at the point x_u solution of $F'(x_u) = u$, the vector field is flowing out $\mathcal{D}$ and hence flowing in this zone for the backward equation, hence $\mathcal{B}$ is flow invariant, hence every solution in this zone does not cross the nullcline, hence goes to infinity with a speed minored by the minimal distance between le nullcline and $\mathcal{B}$.

Hence we have proved that there is a solution going to $-\infty$, and which will spike since the initial condition is below the v-nullcline $\mathcal{N}$. This solution crosses necessarily the line $\{v = v_r\}$, and denote w_L the w associated to this intersection. This solution cuts the phase space in two subspaces which do not communicate: every orbit starting in one of the two subspaces will stay in this subspace. Hence for all $w > w^*$, $\Phi(w) \geq \Phi(w_L)$, hence Φ is decreasing and minored, hence converges to a finite value and presents an horizontal asymptote.

□

We characterized in the case where the subthreshold system has no fixed point the shape of the Poincaré application. In this case, the spiking will necesarilly be of *tonic* type, i.e. the neuron will fire infinitely many spikes (this will be the case whenever $\Phi(\mathcal{D}) \subset \mathcal{D}$). Since the system is a tonic spiking behavior, the study of the Poincaré sequence of iterations of Φ provides a good way to understand the different tonic spiking patterns observed in these models.

3.2 Tonic spiking

As observed numerically in [Touboul, 2008a] and as we can see in figure 8, we can see that the regular spiking is linked with the present in the hybrid system of a generalized limit cycle, the *regular spiking limit cycle*, virtually containing one point at infinity. From a mathematical point of view, this corresponds simply to the convergence of the Poincaré sequence (3.1).

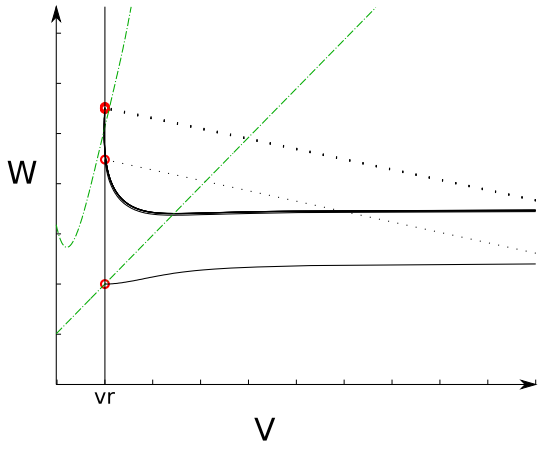

Figure 8: Spiking generalized limit cycle, case of the quartic model. In the simulation, we have cut the trajectories to a given threshold. Threshold has been taken large enough to ensure we simulate the intrinsic system. Green dotted curves represent the nullclines, the red circles the sequence of reset positions, the solid black curves the orbit of the solution of the differential equation and the dotted lines the reset.

The regular spiking behavior is linked with the convergence of the Poincaré sequence to a fixed point. Indeed, if this sequence converges, then the frequency of the spikes will converge also. If it does not, the only way to have spikes regularly corresponds to the case where the ISI map $\mathcal{T}$ is not one-to-one when the Poincaré sequence jumps between the different values corresponding to the same interspike interval. When this case occurs, then one of the point of the cycle is lower than w^* and hence corresponds to a sharp after-potential and the other point is greater than w^* and corresponds to a broad after potential, and the sequence will then be considered as a regular bursting.

The initial conditions and the parameters where the map Φ converges towards its unique fixed point define the regular spiking regions. A necessary condition to have regular spiking is that the fixed point is stable. In this case, the initial conditions w_0 for which the sequence (3.1) converges is given by the attraction basin of this fixed point.

Since we do not have closed form expressions for the map Φ, we provide here sufficient conditions on the dynamics of Φ leading to a regular spiking behavior.

Theorem 3.2. *Assume that $\Phi(w^*) \leq w^*$. Then the sequence of reset positions $(w_n)_{n\geq 0}$ defined in* (3.1) *will converge whatever the initial condition.*

Proof. We first remark that the interval $(-\infty, w^*]$ is stable under the action of Φ. Indeed, Φ is increasing on this interval, therefore for all $w \in (-\infty, w^*]$, $\Phi(w) \leq \Phi(w^*) \leq w^*$. We also note that Φ maps the interval $[w^*, \infty)$ on the interval $(-\infty, w^*]$ since Φ is decreasing

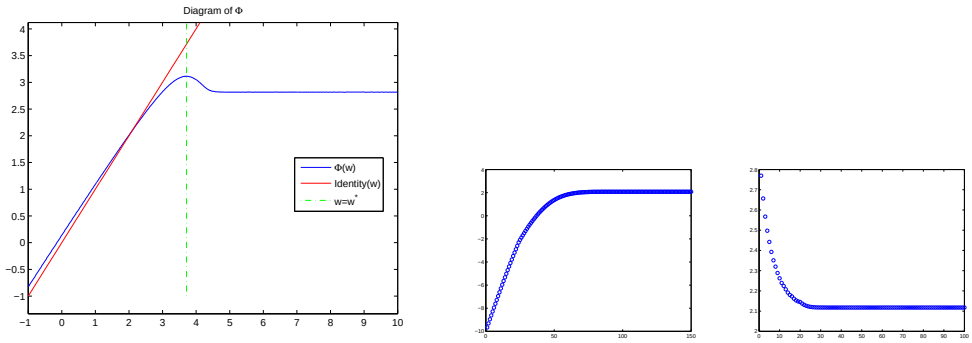

(a) plot of $\Phi(w)$ (b) Sample path of $(w_n) =$ with $w_0 < w^{**}$ (c) Sample path of $(w_n) =$ with $w_0 > w^*$

Figure 9: Convergence towards fixed point.

on this interval, and therefore for all $w \in [w^*, \infty)$, we have $\Phi(w) \leq \Phi(w^*) \leq w^*$. Therefore, is is sufficient to prove that the sequence of iterates of Φ converges on $(-\infty, w^*]$. Eventually we note that in this case we necessarily have $w^{**} < w^*$, since theorem 3.1 ensures us that for all $w < w^**$ we have $\Phi(w) > w$.

On the interval $(-\infty, w^*]$, the sequence $(w_n)_{n\geq 0}$ is monotonous. Indeed, since Φ is increasing on this interval, let $w \in (-\infty, w^*]$ such that $\Phi(w) \leq w$. By an imediate induction on n we have

$$\Phi^{n+1}(w) \leq \Phi^n(w)$$

and hence the sequence is non-increasing. If $\Phi(w) \geq w$, the same argument gives us that the sequence $(w_n)_n$ is non-decreasing.

The subinterval $[w^{**}, w^*]$ is also invariant under the action of Φ since on one hande Φ is increasing on this interval and $\Phi(w^{**}) \geq w^{**}$ using theorem 3.1, and on the other hand $\Phi(w^*) \leq w^*$ by hypothesis. Therefore, the fixed point of Φ is in this interval and the sequence $(w_n)_n$ is a monotonous sequence in a compact set, and hence will necessarily converge to the unique fixed point of Φ.

If $w < w^{**}$ then $\Phi(w) \geq w + d$ and hence there exists an index N such that $w_N \geq w^{**}$, and the previous result applies and gives us the convergence of the sequence.

We conclude therefore that for any initial condition $w \leq w^*$ the sequence converges to the unique fixed point of Φ, and since Φ maps the interval $[w^*, \infty)$ on $(-\infty, w^*]$, for any initial condition in this interval, the sequence (3.1) will converge to the fixed point of Φ. □

The following theorem gives us another sufficient condition on the dynamics to get regular spiking.

Theorem 3.3. *Assume that $\Phi(w^*) \geq w^*$ and $\Phi^2(w^*) \geq w^*$. Then the sequence of reset positions will converge to a fixed point whatever the initial condition.*

Proof. First of all, note that the interval $[w^*, \Phi(w^*)]$ is stable under Φ, since Φ is decreasing on this interval and because of the assumptions of the theorem. Let $w \in [w^*, \Phi(w^*)]$. We have by an imediate induction using that Φ is decreasing on this interval:

$$\begin{cases} \Phi^{2n}(w^*) \leq \Phi^{2n}(w) \leq \Phi^{2n+1}(w^*) \\ \Phi^{2n+2}(w^*) \leq \Phi^{2n+1}(w) \leq \Phi^{2n+1}(w^*) \end{cases}$$

Therefore the study of the sequences $\Phi^{2n}(w^*) =: w^*_{2n}$ and $\Phi^{2n+1}(w^*) =: w^*_{2n+1}$ are essential to characterize the sequence related to any given $w \in [w^*, \Phi(w^*)]$. Let us study theses sequences. We have:

$$w^* \leq \Phi^2(w^*) \leq \Phi(w^*)$$

and therefore by an imediate induction using the monotony of Φ on this interval

$$\Phi^{2n}(w^*) \leq \Phi^{2n+1}(w^*) \leq \Phi^{2n-1}(w^*)$$
$$\Phi^{2n}(w^*) \leq \Phi^{2n+2}(w^*) \leq \Phi^{2n+1}(w^*)$$

Hence the sequence $(w^*_{2n})_{n\geq 0}$ is an increasing and $(w^*_{2n+1})_{n\geq 1}$ is decreasing, and for all n, we have $w_{2n} < w_{2n+1}$. Hence the two sequences converge.

The limit of these sequences is necesarily a fixed point of the map Φ^2. Because of the properties of Φ and the assumptions of the theorem, this map has a unique fixed point, which is the same as the fixed point of Φ. Indeed, because of the shape of Φ, it can either have one or three fixed points. Let $w_1 := \min\{\Phi^{-1}(w^*)\}$. Then Φ^2 is increasing on $(-\infty, w_1)$, decreasing on (w_1, w^*) and increasing again on (w^*, ∞), interval on which the map converges to a finite limit when $w \to \infty$. On $(-\infty, w^*)$, $\Phi^2(w) > w$: it is clearly the case on $(-\infty, w_1)$ and the minimum of Φ^2 is reached at w^* where $\Phi^2(w^*) > w^*$. We therefore conclude that in this case Φ^2 has a unique fixed point, which is necesarily the same as Φ.

Thus the two sequences converge to this same fixed point, and so do any sequence (3.1) having its initial condition in $[w^*, \Phi(w^*)]$.

Let now w_0 be a given initial condition for the sequence (3.1). Necessarily this sequence w_n will be in the invariant interval $[w^*, \Phi(w^*)]$ after a finite number of iterations. Indeed, assume that $w_0 < w^*$. The sequence cannot be upperbounded by w^* since there is no fixed point in $(-\infty, w^*)$. Hence there will be an integer p such that $\Phi^p(w_0) \leq w^*$ and $\Phi^{p+1}(w_0) \geq w^*$. Then because of the monotony of Φ we have $\Phi^{p+1}(w_0) \leq \Phi(w^*)$. If $w_0 \geq \Phi(w^*) > w^*$, then because of the monotony of Φ we have $\Phi(w_0) \leq \Phi(w^*)$ and hence the related sequence converges because of the properties already proved. □

We have identified two simple sufficient conditions on Φ to obtain a regular spiking behavior. These criteria are not directly related to the parameters of the model, but they will be useful in order to understand mathematically the dependency with respect to the

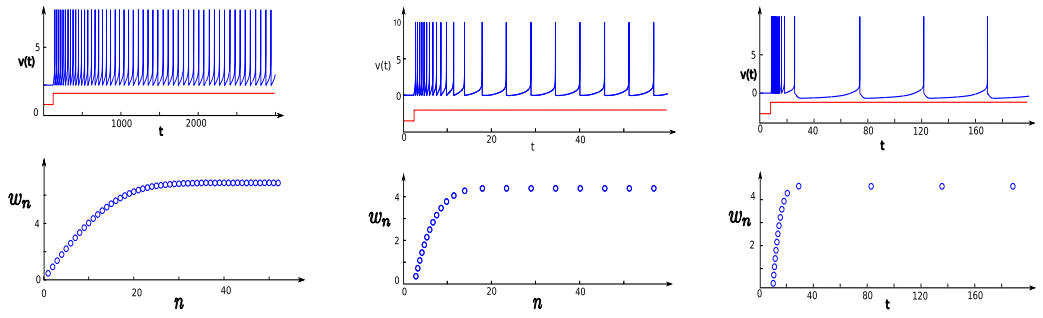

(a) Spike Frequency Adaptation (multiplier 0.355)

(b) Intermediate case (multiplier 0.068)

(c) Mixed Mode (multiplier 10^{-4})

Figure 10: Different types of convergence for the quartic model, when all the parameters are fixed but the time scale of the adaptation variable a. The faster the adaptation is, the slower the convergence is.

parameters as did in section 3.5, and also that can be easily used in numerical simulations to compute the zones of parameters corresponding to this regular spiking behavior, as we do in section 5.5.

This analysis accounts for the stationary spiking behavior, and does account for the transient phase, i.e. before the convergence of the sequence. In the spike patterns analysis, we generally distinguish between two types or regular spiking: the spike frequency adaptation that corresponds to the case where the spike frequency smoothly converges to its stationary value, and mixed mode where the neuron transiently fires fast few spikes before reaching its stationary spike frequency. From the biological point of view, the distinction between these behaviors is not so clear, and we can continuously go from one behavior to the other. The differences between these behaviors simply corresponds from a mathematical point of view to the way the sequence of iterates converges towards the fixed point (see Fig.10), and we can quantify in our framework this convergence rate, which is directly linked with the multiplier of the fixed point (the value of the derivative of Φ at the fixed point). If the absolute value of this multiplier is very small (close to 0), then the convergence will be very fast, and we will see a short transient before the regular spiking, and hence we will have a mixed mode (see Fig. 10(c)). If the multiplier modulus is close to 1, then the convergence will be very slow, and we will have spike frequency adaptation (see Fig. 10(a)).

3.3 Tonic Bursting

In this case, we observed numerically in [Touboul, 2008a] and as we can see in figure 11, the bursting activity is linked with the existence of a generalized limit cycle of the hybrid system, the *bursting limit cycle*, virtually contining many points having an infinite membrane

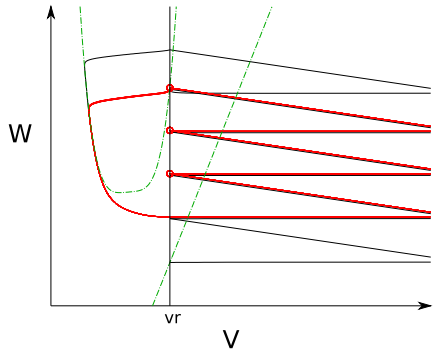

Figure 11: Bursting generalized limit cycle. In the simulation, we have cut the trajectories to a given threshold high enough to approximate the behavior of the intrinsic system. The red curve corresponds to the bursting limit cycle, and the red circles the reset locations on this cycles. The black trajectory is the transient phase, and the green dotted curves correspond to the nullclines of the system.

potential. The regular bursting behavior, whatever the transient behavior, is linked with the presence of such a cycle, and this cycle corresponds exactly to periodic points for the the Poincaré map Φ.

We can provide here a condition for having cycles of any period. Indeed, one of the simplest application of Sarkovskii's theorem (see e.g. [Devaney, 2003]) is that if there exist a periodic point of period 3, then there exist periodic points of any period, hence bursts with any number of spikes per burst. Theorem 3.4 gives us a simple criterion on the dynamics of Φ to have a period 3 cycle.

Theorem 3.4 (Cycles of any period)**.** *Let* $w_1 := \min\{\Phi^{-1}(w^*)\}$. *Assume that:*

$$\begin{cases} \Phi(w^*) > w^* \\ \Phi^2(w^*) < w_1 \\ \Phi^3(w^*) > w^* \end{cases} \tag{3.5}$$

Then there exists a non-trivial period 3 cycle, hence the reset process has cycles of any period.

Proof. The only thing to prove is that there exist a real T such that

$$\begin{cases} \Phi^3(T) = T \\ \Phi(T) \neq T \end{cases}$$

We know that there exists a unique fixed point of Φ, which we denote w_∞ and which lies in the interval $[w^*, \Phi(w^*)]$. Here we prove that there exists another solution of $\Phi^3(x) = x$. Indeed, let us describe the function Φ^3:

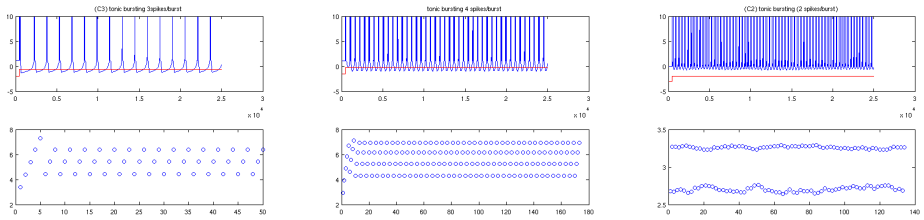

(a) Period three point (b) Period four point (c) Period two point

Figure 12: Different types of bursts and the periodic orbits of Φ associated. The last example of a point of period two shows that the system is quite excitable. Indeed, the precision of our integration scheme is very high in this case. This irregularity we observe is linked with numerical errors associated with the excitability of the system: we are very close of the disappearance of this cycle.

- It is increasing on $(-\infty, w_2)$ where $w_2 = \min\{\Phi^{-2}(w^*)\}$, and above the curve $y = x$ on this interval.

- decreasing on (w_2, w_1) and $\Phi^3(w_1) = \Phi^2(w^*) < w_1$ hence the curve crosses once the curve $y = x$, at a point strictly inferior to w^*.

Hence we have proved that there exists a period 3 cycle. Sarkovskii's theorem (see e.g. [Devaney, 2003]) ensures us that there are cycles of any period for the map Φ . □

Remark 1. This theorem gives us a quite simple condition on Φ to get period 3 cycles. This implies that the system is chaotic, as shown in the excellent paper of Li and Yorke [Li and Yorke, 1975]. Nevertheless the chaos they find is a topological chaos. It means that the set of cycles is dense. It does not corresponds to the usual definition of chaos used in neuroscience, understood as sensitive dependency on initial conditions.

Conditions such as the one given in theorem 3.4 can be found for any period. The difficulty is to prove that these conditions are satisfied, since we have no closed form expression for the map Φ, and in this case numerical simulation is helpfull. As we will see in section 3.5, the system will undergo a period-adding bifurcation in function of the reset value of the membrane potential, and therefore bursts of many periods will be observed.

3.4 Multistability

In section 3.2, we gave sufficient conditions on the map Φ for the convergence of the sequence (3.1) to the fixed point of Φ whatever the initial condition. These theorems imply

in particular that the fixed point of Φ is stable. Nevertheless, in the case where the map Φ is not completely contracting, i.e. when

$$\max_{v\in\mathbb{R}} |\Phi'(v)| > 1$$

it is possible to have multistable behaviors. Indeed, except in the cases covered by the theorems of section 3.2, different types of behavior can appear depending on the initial condition of the sequence (3.1). For instance, the map Φ can have a stable fixed point and the map Φ^2 two other stable fixed points. In that case, we can observe either a regular spiking when the initial condition of the Poincaré sequence is contained in the attraction basin of the stable fixed point of Φ, or a regular bursting with two spikes per burst in the case where the initial condition of the Poincaré sequence is in the attraction basin of the cycle.

3.5 Dependency on the parameters

We have seen that in the case where the subthreshold dynamics has no fixed point can correspond to tonic spiking, tonic bursting, or both at the same time depending on the initial condition. The question we address in this section is to characterize the dependency of the system with respect to the parameters of the model, and the bifurcations from one behavior to the other.

3.5.1 Bifurcations in the spike-triggered adaptation parameter

The parameter having the simplest effect on the dynamics is the adaptation parameter d: it simply shifts vertically the Poincaré map, and does not change its shape. This simple behavior allows us to understand qualitatively the changes in the behavior of the Poincaré sequence.

Therefore, if the Poincaré map is globally contracting, we will not observe bifurcations in the parameter d, and the system will always converge to the unique fixed points, which increases when increasing d. We denote this fixed point $w_{fp}(d)$.

If the map is not globally contracting, bifurcations can appear with respect to the parameter d. Denote by I_1 the zone where the derivative of Φ is greater than 1 in absolute value. This interval is a bounded interval fully included in $[w^*(d), \infty)$, because of the convexity assumption and the presence of the plateau that implies that the derivative of Φ with respect to w tends to 0. As stated, since the shape of Φ does not depend on d, I_1 do not depend on d either.

If $w_{fp}(0) > \max I_1$, then the fixed point of the system is always stable for all $d > 0$ and there is no bifurcation in d.

If $w_{fp}(0) \in I_1$, we denote by $d_1 = \inf\{d > 0; w_{fp}(d) \neq I_1\}$. The fixed point will be unstable and the neuron will be bursting or chaotically spiking while $d < d_1$, and for $d > d_1$, the fixed point becomes stable and the neuron will fire regularly . At the point where $d = d_1$, the fixed point will have a multiplier equal to -1, and the map undergoes a period doubling

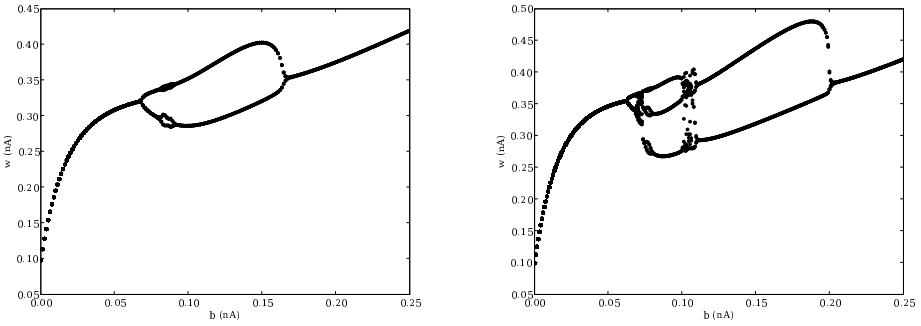

(a) $V_r = -48.2mV$ (b) $V_r = -47.7mV$

Figure 13: Orbits of Φ for different initial conditions, varying the spike-triggered adaptation parameter d, in the case of the dimensioned Adaptive Exponential model. We can observe that for d small enough the system converges towards the fixed point of Φ. When increasing d, as described in the text, the fixed point loses stability via a period doubling bifurcation and a cycle of period 2 appears. In the case (a) the system presents another period doubling bifurcation for $d \approx 0.8$, and then returns to equilibrium via an inverted period doubling bifurcation as described in the text. In the second simulation for V_r larger,

bifurcation provided that the genericity and the transversality conditions are satisfied (see e.g. [Kuznetsov, 1998, section 4.5]). The transversality condition is always satisfied since $\frac{\partial^2 \Phi}{\partial w \partial d} \equiv 1$ and hence never vanishes. The genericity condition reads:

$$\frac{1}{2}\left(\frac{\mathrm{d}^2\Phi}{dw^2}\right)^2 + \frac{1}{3}\frac{\mathrm{d}^3\Phi}{dw^3} \neq 0 \tag{3.6}$$

This condition is quite difficult to check since we do not have a closed form for the map Φ, but the value of (3.6) can be numerically computed quite easily.

If $w_{fp}(0) < \min I_1$, we similarly define $d_1 = \inf\{d > 0, w_{fp} \in I_1\}$ and $d_2 = \sup\{d \geq d_1, w_{fp} \in I_1\}$. The system will undergo a period doubling bifurcation at the point $w^*(d_1)$ for $d = d_1$ and a period doubling bifurcation at the point $w^*(d_2)$ for $d = d_2$ provided that the genericity condition (3.6) is satisfied. For $d \in (d_1, d_2)$, the system do not have a stable fixed point. It can emit bursts, or even have a chaotic behavior in this zone (see figure 13).

3.5.2 Stabilization by the input current

First of all, we are interested in the effect of the input current. Indeed, increasing the input from the value $I = -m(b)$ will let the system in the parameter zone where there is no fixed point, and decreasing it will make the system switch to the case where there are two fixed

points treated in section 4. In this section we are interested in the effect of increasing the input current.

Interestingly, increasing the input current has a stabilizing effect on the behavior of the neuron: we prove in theorem 3.5 that for I large enough the Poincaré sequence will always converge to a fixed point. Nevertheless, the complexity we described in the previous sections will clearly affect the dynamics when we vary I. Note that this type of behavior is what is sometimes called fast spiking behavior.

Theorem 3.5. *Let a, b, v_r, d be fixed parameters. There exists I_s such that for all $I > I_s$ the sequence of iterates of Φ converges.*

Proof. The proof of this theorem is based on the changes induced by increasing the current around the point (v_r, w^*). We prove that increasing I enough will lead the system in the case of theorem 3.2, which will conclude the proof.

The point w^* depends on I, and therefore we denote it $w^*(I)$ in this proof for the sake of clarity. At this point $(v_r, w^*(I))$, the vector field in the direction of v does not change when increasing the input current, by the vector field in the direction of the adaptation variable w it decreases proportionaly to I (i.e. increasing I by δI amounts adding $-\delta I$ to the vector field in the direction of w). This new dynamical system can be readily deduced from the original one changing w in $\tilde{w} = w - I$. Using this change of variable, we have $\tilde{w}^* = F(v_r)$ and the new Poincaré map reads:

$$\tilde{\Phi}(\tilde{w}) = \Phi(\tilde{w} + I) - I,$$

and the condition of theorem 3.2 simply reads $\tilde{\Phi}(\tilde{w}^*) \leq \tilde{w}^*$. In the plane $(u, \tilde{w})$ with $u = (v - v_r + 1)^{-\varepsilon/2}$, the equation of the trajectory reads:

$$\frac{\mathrm{d}\tilde{W}}{\mathrm{d}u} = -\frac{2a}{\varepsilon u^{1+2/\varepsilon}} \frac{bu^{-2/\varepsilon} + \beta - \tilde{W} - I}{F(u^{-2/\varepsilon} + v_r - 1) - \tilde{W}}$$

and the limit at zero of the solution (which exists because of the assumptions) satisfies the equation:

$$\begin{aligned}
\tilde{W}(0,1,I) &= F(v_r) + \int_0^1 \frac{2a}{\varepsilon z^{1+2/\varepsilon}} \frac{(bz^{-2/\varepsilon} + \beta - \tilde{W}) - I}{F(z^{-2/\varepsilon} + v_r - 1) - \tilde{W}}\, dz \\
&= F(v_r) + \int_0^1 \frac{2a}{\varepsilon z^{1+2/\varepsilon}} \frac{(bz^{-2/\varepsilon} + \beta - \tilde{W} + m(b))}{F(z^{-2/\varepsilon} + v_r - 1) - \tilde{W}}\, dz \\
&\quad - 2\,a\,(I + m(b)) \int_0^1 \frac{1}{\varepsilon z^{1+2/\varepsilon} (F(z^{-2/\varepsilon} + v_r - 1) - \tilde{W})}\, dz
\end{aligned}$$

Hence there exists $I_s > -m(b)$ such that for all $I > I_s$ we have $\tilde{W}(0,1,I) + d < F(v_r)$. This is equivalent to the condition of theorem 3.2, therefore for all $I > I_s$, the system will be in a regular spiking behavior.

□

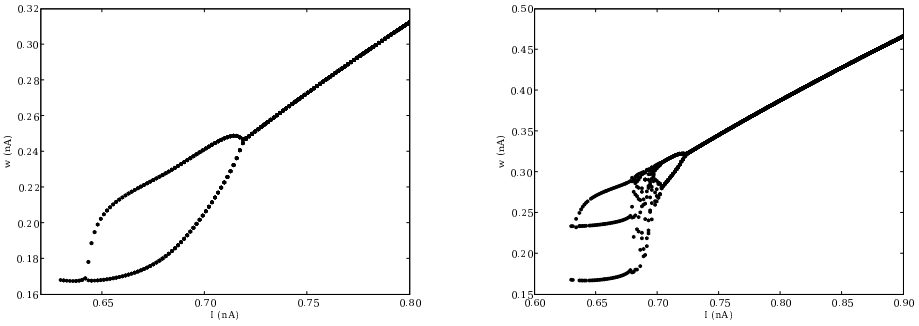

(a) $V_r = -48.2mV$ (b) $V_r = -47.7mV$

Figure 14: Orbits of Φ when varying the input current I in the case of the dimensioned Adaptive Exponential model. In the case 14(a) the reset location is small enough and the dynamics only presents a loss of stability via period doubling and then returns to equilibrium. In the second case 14(b), the fixed point is unstable when it appears and we have a period two cycle immediately followed by a period 3 cycle, then via an inverted period-adding bifurcation we return to a period two cycle, and then by inverted period doubling bifurcation to the fast-spiking equilibrium. The transition from period three to period two presents a chaotic behavior.

Therefore, we can see that increasing the input current has a stabilizing effect on the dynamics. We present in figure 14 some numerical results illustrating this stabilization effect in the case of the exponential integrate-and-fire model. We observe for two different values of v_r that the system undergoes bifurcations with respect to the input current, sometimes involving chaotic spiking, but after a given value of the input current, the system spikes regularly, and the Poincaré sequence converges towards its fixed point.

3.5.3 Cascade of period adding bifurcations and chaos with respect to v_r

A very interesting bifurcation parameter is the reset value of membrane potential v_r. The dependency of the Poincaré application with respect to this parameter is very intricate. The effect of increasing the reset value sharpens the Poincaré application, and therefore destabilizes the possible stable fixed point or stable cycles. This qualitative observation is confirmed by numerical simulations. In the case of the exponential model, for v_r small enough, the Poincaré application is smooth, because of the slope of the exponential function for small v values tends to zero. But in the case of the quartic model, decreasing v_r also sharpens F because of the fast divergence of the quartic function.

We provide in figure 15 a graph of the stationary Poincaré sequence (i.e. removing the transient phase) as a function of the reset voltage v_r corresponding to the quartic

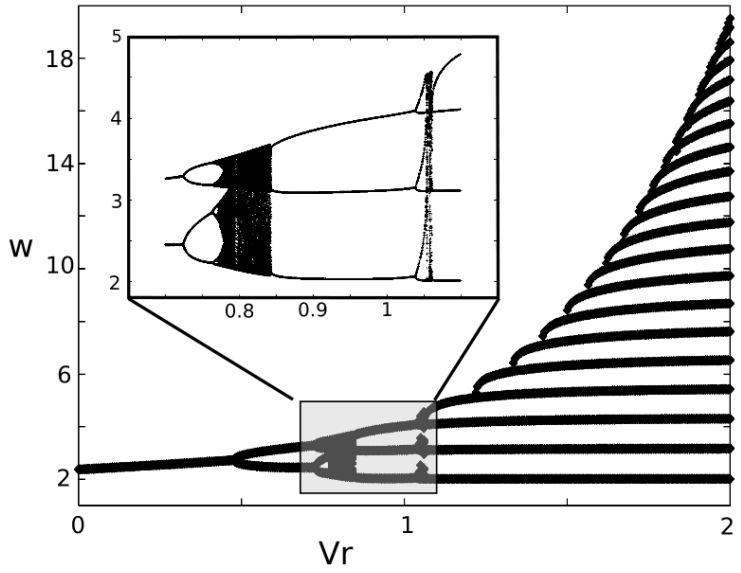

Figure 15: The period adding bifurcation cascade in the Poincaré sequence for the quartic model, $a = 0.03$, $b = 0.7$, $d = 1.15$, and $v_r \in [0, 2]$, and a zoom on the transitions from period 2 to period 3 and period 3 to period 4.

model. A similar diagram was given in the case of the adaptive exponential model in [Touboul and Brette, 2008]. We observe that the system present sharp transitions from rest (regular spiking) to cycles of period two (bursts with two spikes per burst) via a period doubling bifurcation, and from cycles of period n to cycles of period $n + 1$ for $n \geq 2$ via period adding bifurcations involving chaotic spiking regions.

4 Existence of fixed points

In the case where $I < -m(b)$, the system has two fixed points, one of which is always a saddle fixed point. We already studied in section 2 the stable manifold of this saddle fixed point, and explained in the cases where there exists stable closed orbits (fixed points of periodic orbit) how this manifold shaped the related attraction basin.

This stable manifold is essential for characterizing the definition domain and the the dynamics of Φ on this domain. The map Φ will only be defined on the line $\{v = v_r\}$ for values of w such that (v_r, w) is neither in the attraction basin of the possible closed orbit nor on the stable manifold of the saddle fixed point.

4.1 Case $\mathcal{D} = \mathbb{R}$

We are first interested in the cases where the reset line $\{v = v_r\}$ neither crosses the saddle manifold nor the attraction basin of the possible stable fixed point. We know that the SMSFP is the graph of an unbounded increasing function of v for $v \geq v_+$. Therefore, the cases where the stable manifold do not cross the line $\{v = v_r\}$ necesarilly correspond to the cases where the stable manifold is fully included in a half plane $\{v \geq v_{\min}\}$. This corresponds to the cases where:

- the subthreshold system has two unstable fixed points and no stable limit cycle (Figs. 3(a) and 3(b)).
- there exists an unstable limit cycle circling the stable fixed point (Fig. 2(a))
- or when the stable manifold crosses both nullclines (Fig. 2(b)).

In these cases, for all $v_r \leq v_{\min}$, the line $\{v = v_r\}$ will not intersect the SMSFP nor any possible attraction basin. Therefore, the Poincaré application Φ is defined on $\mathbb{R}$ and the proof of theorem 3.1 readily extends to this case. Hence in that case Φ is a regular map increasing and concave on $(-\infty, w^*]$ and decreasing on $[w^*, \infty)$, having a unique fixed point, an horizontal asymptote at infinity and such that $\Phi(w) \geq w + d$ for all $w \leq w^**$. Since the map Φ is defined on $\mathbb{R}$ (and therefore $\Phi(\mathcal{D}) \subset \mathcal{D}$, will either be at rest and fire no spike (if there exists a resting state: stable equilibrium or stable periodic orbit) or in a tonic spiking behavior. In the tonic spiking case, since the map satisfies the same properties as one of the case where the subthreshold system has no fixed point, theorems 3.2, 3.3 and 3.4, and the firing can either correspond to chaotic spiking, regular spiking or regular bursting, depending on the parameters of the system.

4.2 Case $\mathcal{D} = \mathbb{R} \setminus \mathcal{A}$ where $\mathcal{A}$ is a countable set

The cases where the reset line crosses the SMSFP but not any attraction basin of SSO is more intricate. It corresponds to the cases where:

- the subthreshold system has two unstable fixed points and no stable limit cycle, and $v_r \geq v_{\min}$ and $v_r \neq v_-$. (cases of Figures 3(a) and 3(b))
- the subthreshold system presents a stable fixed point and an unstable periodic orbit. In that case let us denote by $v_{p,\max}$ (respectively $v_{p,\min}$) the maximal (respectively minimal) value of the variable v or the periodic orbit. The line $\{v = v_r\}$ crosses the stable manifold but not the attraction bassin when $v_{\min} \leq v_r < v_{p,\min}$ or $v_r \geq v_{p,\max}$.

In these two cases, the reset line $\{v = v_r\}$ has finitely many intersections with the stable manifold, and we denote by $\mathcal{A}$ the set of intersection points. The map Φ is defined on $\mathbb{R} \setminus \mathcal{A}$. This set is a finite union of open intervals. On each interval, the map Φ satisfies the properties given in theorem 3.1. The of the orbits of the differential system (1.1) around these intersection points completely changes because of the property that the orbits cannot

cross the stable manifold, and therefore at each intersection point with the saddle manifold the map Φ undergoes jumps. Hence when the stable manifold oscillates around the fixed point, the map Φ will have arbitrary many discontinuity points.

If $v_r > v_+$ then the map Φ will have a unique point where it is undefined, for $v_r > v_-$, an even number of such points, and for $v_{\min} < v_r < v_-$, an odd number. For $v = v_-$, the system will have an infinite countable number of discontinuities, composed of two sequences $(m_i,\ i \in \mathbb{N})$ such that $m_i < w_-$, is increasing and converges to w_- and $(M_i,\ i \in \mathbb{N})$ such $M_i > w_-$, the sequence is decreasing and converges to w_- (see diagram 16).

The dynamics of Φ in this region of parameters will therefore be very complex. It can have multiple fixed points, no fixed point, and the map is discontinuous.

We denote by $\mathcal{A}$ the set of intersections of the reset line with the stable manifold of the saddle fixed point. The set of adaptation values such that the system will be in a phasic spiking state (i.e. fires finitely many spikes) is given by:

$$(P) = \bigcup_{n=0}^{\infty} \Phi^{-n}(\mathcal{A})$$

- If $v_r < V_{\min}$, then Φ is defined on $\mathbb{R}$ and the analysis done in the case where there is no fixed point applies directly.
- If there is no fixed point for the map Φ (for instance if the identity line crosses the discontinuity), then regular spiking is impossible, and hence we will have bursts or irregular spiking necessarily.
- If there is a unique fixed point, then regular spiking and bursts can coexist depending on the initial condition. Indeed, the map Φ is discontinuous and can present stable cycles together with the presence of a stable fixed point. For instance assume that $v_r < v_+$. In this case, denote by w_d is the discontinuity point (the intersection of $v = v_r$ with the stable manifold of the saddle fixed point). We have $w_d < w^*$. If furthermore $\Phi(w_d^-) < w_d$, then the image of (w_d, ∞) by Φ is included in $(-\infty, w_d)$ which is stable under the action of Φ. Hence the dynamics of Φ is after possible one iteration described by the dynamics of Φ on $(-\infty, w_d)$. It is easy to prove that in this case the sequence converges towards the fixed point of Φ. This proof readily extends to the case where $v_r > v_+$ and $\sup_{x \in (-\infty, w_d)} \Phi(x) < w_d$.
- The case where there are many fixed points is way more complex. In this case the system could have different regular spiking frequencies, depending on the initial condition. In this case of multiple attractors, the system could switch between these attractors, be chaotic, present hysteresis, and its computational capabilities are increased as well as its sentivity.

4.3 Phasic behaviors

In this section, we consider the cases where the reset line intersects the attraction basin $\mathcal{B}$ of a stable closed orbit and by $\mathcal{C}$ the stable manifold of the saddle fixed point. The set of

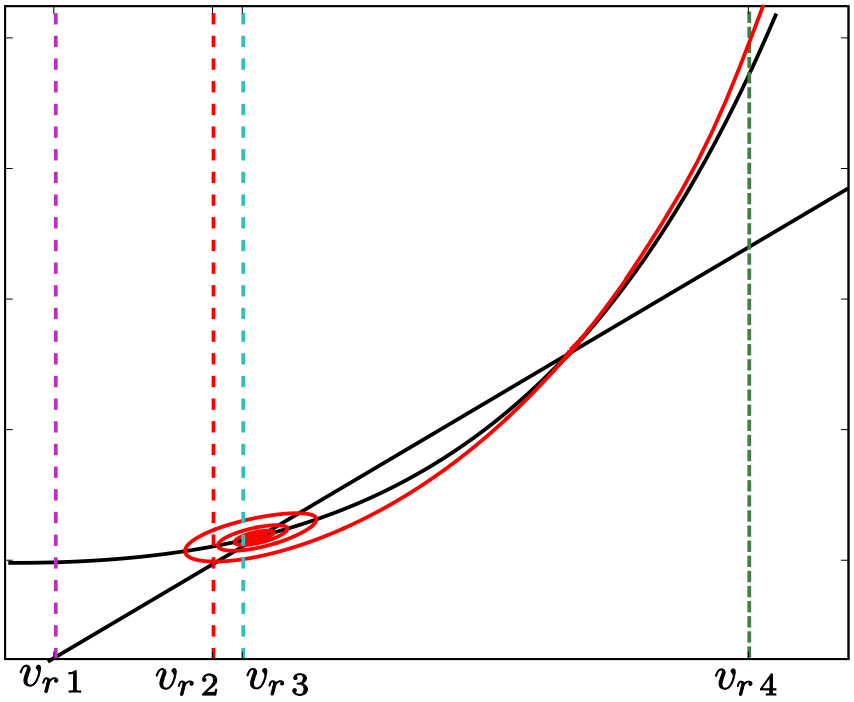

(a) Nullclines and different reset locations v_{r1}, v_{r2}, v_{r3}, v_{r4} corresponding to different qualitative behaviors for the map Φ.

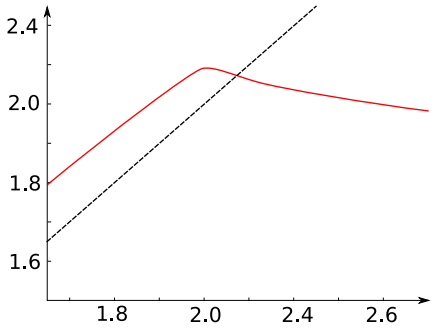

(b) $v_r = v_{r\,1}$: Φ is continuous

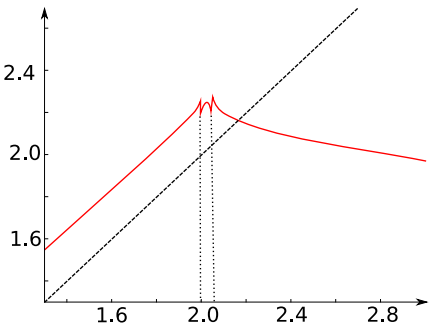

(c) $v_r = v_{r\,2}$: 2 discontinuity point

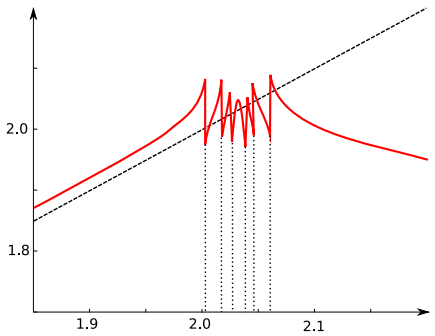

(d) $v_r = v_{r\,3}$: 6 discontinuity point, 7 fixed points

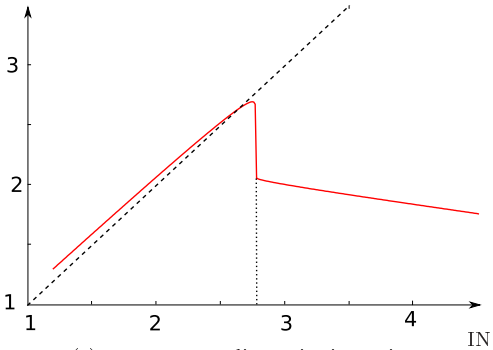

(e) $v_r = v_{r\,4}$: 1 discontinuity point

Figure 16: Case of two unstable fixed points for the classical adaptive exponential model. Phase plane and graph of the map Φ for different values of v_r, for the same set of parameters.

adaptation values that do not lead to system to fire is given by:

$$\mathcal{A} = \{w \in \mathbb{R}\ ;\ (v_r, w) \in \mathcal{B} \text{ or } (v_r, w) \in \mathcal{C}\}\,.$$

Therefore, definition domain of the Poincaré application in this case is

$$\mathcal{D} = \mathbb{R} \setminus \mathcal{A},$$

and the set of initial conditions corresponding to a phasic spiking (i.e. emission of a finite number of spikes) is given by

$$(P) = \bigcup_{n=0}^{\infty} \Phi^{-n}(\mathcal{A})$$

and the complementary of this set corresponds to the tonic spiking cases.

To study further the behavior of the system in this case, we discuss different cases depending on the shape of the stable manifold and the position of v_r with respect to the fixed point v_+. Interestingly, the shape of the stable manifold only depends on the parameters of the subthreshold system.

4.3.1 The stable manifold does not cross the v-nullcline

We first consider the case where the manifold Γ^- does not cross the v-nullcline.

For $v \leq v_+$, two cases can be distinguised:

- In the case where the Γ^- intersects no nullcline (case of figure 2(c)), the definition domain $\mathcal{D}$ is an open interval $(-\infty, w_{\max}(v_r))$ such that $w_{\max}(v_r) < \min(w^*, w^{**})$. On this interval, the proof of theorem 3.1 can be applied and we obtain that Φ is increasing and that $\Phi(w) \geq w + d$ for all $w \in \mathcal{D}$. Therefore, provided that $d > 0$, there exists $N \geq 0$ such that $\Phi^N(w) > w_{\max}(v_r)$. This implies that the neuron starting from any initial condition (v_r, w) such that $w \in \mathcal{D}$ will fire a finite number of spikes and then returns to equilibrium (fixed point of stable periodic orbit).

- When manifold Γ^- crosses only the w-nullcline (case of figure 2(d)), the definition domain is also an open interval $(-\infty, w_{\max}(v_r))$. Let us define the interval $I = [v_1, v_2]$ such that the stable manifold is below the two nullclines. We have $v_1 \leq v_-$ and $v_2 \geq v_+$. For $v_r \in I$, the neuron will necesarily fire finitely many spikes and return to rest from the spiking point of view, as we proved in the latter case. For $v_r < v_1$, we have $w^{**} < w_{\max}(v_r) < w^*$. Therefore the map Φ will be increasing on $\mathcal{D}$. If $\Phi(w_{\max}) \leq w_{\max}$, then there exists a fixed point for the map Φ, which will be stable, we can easily prove (the proof is essentially the same as the one of theorem 3.2) that the Poincaré sequence will converge to the fixed point of the map Φ. In this case the system presents a bistable behavior (see figure 18): there exists a stable subthreshold behavior and a stable spiking behavior that coexist. If $\Phi(w_{\max}) > w_{\max}$, because of the convexity property (which can be proved exactly the same way as in theorem 3.1), there exists $\varepsilon > 0$ such that $\Phi(w) - w \geq \varepsilon$ and therefore the system will return to rest

after firing finitely many spikes. Therefore the whole behavior of Φ depends on the sign of $\Phi(w_{\max}(v_r)) - w_{\max}(v_r)$.

These two cases are very similar for $v > v_+$. Indeed, in that case, the manifold Γ^+ delineating the attraction basin of the nonspiking trajectory is the graph of an increasing function of v, and is above the two nullclines. The definition domain of the Poincaré application is here again an open interval $(-\infty, w_{\max}(v_r))$ with $w_{\max}(v_r) > \max(w^*, w^{**})$.

- In the case where $\Phi(w_{\max}(v_r)) > w_{\max}(v_r)$ we are able to define $\varepsilon > 0$ such that $\Phi(w) - w \geq \varepsilon$ and the system will be in a phasic spiking behavior.
- In the case where $\Phi(w^*) < w_{\max}(v_r)$, then we have $\Phi(\mathcal{D}) \subset \mathcal{D}$ and therefore the system will fire infinitely many spikes. Depending on the properties of the map Φ, the system can either spike regularly (when the fixed point is stable), emit bursts of chaotic spike patterns.
- In the case where $\Phi(w^*) \geq w_{\max}(v_r)$, we do not have $\Phi(\mathcal{D}) \subset \mathcal{D}$. In this case, $\mathcal{D}$ can be separated into two different sets that can have quite intricate shapes: a set of values of the adaptation variable where the neuron fires finite many spikes and a set where the neuron fires infinitely many spikes. To study these sets, we define

  $$P_1 = \{w \in \mathcal{D} \ ; \ \Phi(w) \geq w_{\max}(v_r)\}$$

  This set corresponds to the set of adaptation values w such that $\Phi(w) \notin \mathcal{D}$ and hence that will fire one spike and then return to a subthreshold stable orbit. We then define recursively the set $P_{n+1} = \Phi^{-1}(P_n)$ of initial conditions such that the neuron will fire exactly n spikes before beeing attracted by the stable subthreshold orbit. The set of phasic spiking initial conditions is therefore defined by

  $$P = \bigcup_{n=1}^{\infty} P_n,$$

  and the set of tonic spiking is $\mathcal{D} \setminus P$. In figure 17 we represented the construction of these two sets untill T_3, and we observe the complexity of the set we will obtain. If the fixed point is stable, both the tonic spiking and the phasic spiking sets will be a countable union of non-empty intervals, and the Poincaré sequence will jump from one interval to the other untill reaching the attraction basin of the fixed point of Φ, where they keep trapped. If the fixed point is unstable, the tonic spiking set will be composed of a countable points, which are the consecutive reciprocal images by Φ of the unstable fixed point. Therefore the neuron will not present cycles. In this case, the behavior of Φ strongly depends on the initial condition.

4.3.2 Unbounded stable manifold crossing the v-nullcline

If the stable manifold crosses the v-nullcline as in figure 2(b), then for each $v \geq v_{\min}$ the reset line will intersect the attraction bassin on a bounded interval $(w_{\min}(v_r), w_{\max}(v_r))$ and

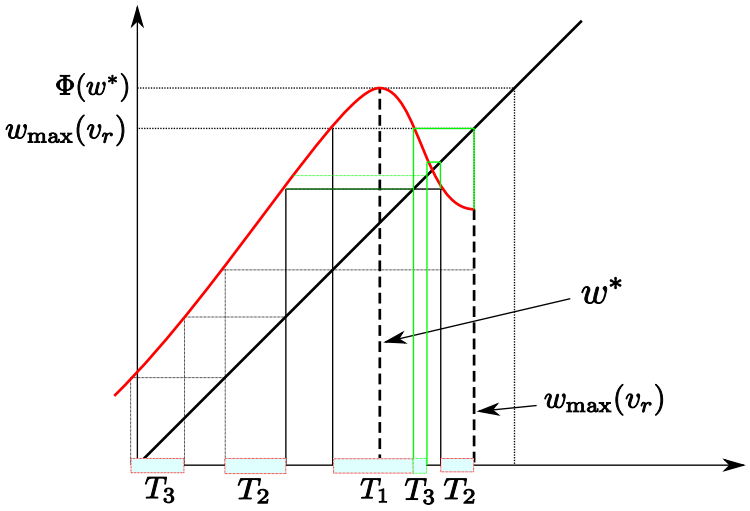

Figure 17: Construction of the phasic spiking set, for two iterations. The red curve is the map Φ and the black line the identity map. The green construction line correspond to the contribution of the set T_2 for $w > w^*$ to T_3.

the definition domain of the Poincaré application is the union of two semi-infinite intervals:

$$\mathcal{D} = (-\infty, w_{\min}(v_r)) \cup (w_{\max}(v_r), \infty) =: I_1 \cup I_2.$$

Furthermore any orbit starting from (v_r, w) with $w \in I_2$ will cross the reset line on I_1 after a finite time, and therefore we have $\Phi(I_2) \subset \Phi(I_1)$. Because of the shape of the separatrix, there exists $v_{\min} < v_1 < v_-$ such that on (v_1, v_+) we have $w_{\min}(v_r) < \min(w^*, w^{**})$

- If $\sup_{w \in I_1} \Phi(w) \in [w_{\min}(v_r), w_{\max}(v_r)]$, the system will fire finitely many spikes.

  Indeed, if $v_{\min} < v_r < v_1$, for all $w \in I_1$ we have $w + d \leq \Phi(w) \leq w_{\max}(v_r)$, and therefore the Poincaré sequence is strictly increasing and will necessarily end up in the attraction basin or on the stable manifold, and hence stops firing.

  If $v_r < v_1$ or $v_r > v_+$, there exists $\alpha > 0$ such that $\sup_{w \in I_1} \Phi(w) - w \geq \alpha$ and therefore any orbit will be in the attraction basin of the SSO and will stop firing after a given number of spike fired.

  For any initial condition $w \in I_2$ we have $\Phi(w) \subset \Phi(I_1)$ and therefore either $\Phi(w)$ is in the attraction basin of the subthreshold equilibrium, or it is in I_1 and the above analysis applies and the system is in a phasic spiking mode.

- If $\sup_{w \in I_1} \Phi(w) < w_{\min}(v_r)$, then necessarily $\Phi(I_1) \subset I_1$ and the map Φ has a fixed point in I_1. Furthermore, we have $\Phi(\mathcal{D}) \subset I_1$ and therefore the system will be in a

tonic spiking behavior. If $v_r \leq v_+$, we have $w_{\min} < w^*$, the fixed point is attracting and all the Poincaré sequences converge to this fixed point (see proof of theorem 3.2). If $v_r < v_+$, the type of tonic spiking depends on the properties of the map, the system will possibly fire chaotic, regular or bursting patterns.

- If $\sup_{w \in I_1} \Phi(w) > w_{\max}(v_r)$, then there exists an interval $J \subset \mathcal{D}$ such that all the trajectory with initial condition (v_r, w) with $w \in J$ will stop firing after one spike. We can build the phasic and the tonic subspaces of $\mathcal{D}$ recursively as we did in the previous case. The shape of this set can be quite complex, and the behavior of the Poincaré sequence depends on the initial condition on this set.

4.3.3 Bounded attraction basin

In the case where there exists an unstable periodic orbit in the system, we have seen that the attraction basin of the stable fixed point was bounded, delineated by this periodic orbit, and that the stable manifold winds around this orbit. In this case, let us denote by $v_{\min}$ the minimal value of the membrane voltage on the cycle and by $v_{\max}$ its maximal value. The behavior of the system for $v_r \in (v_{\min}, v_{\max})$ is very complex. Indeed, the reset line will cross the attraction basin on an interval of values for the adaptation $(w_{\min}, w_{\max})$, but since the stable manifold, since it oscillates around the orbit converging to it, there is a countable sequence of intersection points of the reset line with the stable manifold: $(m_i, i \in \mathbb{N})$ converging to $w_{\min}$ and $(M_i, i \in \mathbb{N})$ converging to $w_{\max}$. At each of this point the map Φ is undefined and there is a jump of the values of the map Φ at these points. Hence the definition domain of the map Φ has a quite complex shape, and Φ an intricate discontinuous dynamics on it.

For $v > v_{\max}$ the reset line will cross the stable manifold on a finite set of adaptation values, and at these points the map Φ is undefined and jumps. This case can be studied as the case of two unstable fixed points and no stable periodic orbits treated at the beginning of the section.

5 Discussion

5.1 Phasic behaviors

We have seen that in many cases when there exists stable subthreshold orbits that the system can fire finitely many spikes before converging to this subthreshold orbit. These behaviors are known as *phasic behaviors*. In [Touboul, 2008b, Izhikevich, 2003, Brette and Gerstner, 2005], the authors distinguished between two main types of phasic behaviors : phasic spiking and phasic bursting. In our framework, the phasic spiking corresponds to the case where the neuron only fires a spike before returning to rest, which corresponds for instance to the set $\mathcal{T}_1$ of figure 17, and the phasic burstings to the the rest of the phasic set, in which case the neuron fires few spikes before returning to its subthreshold equilibrium.

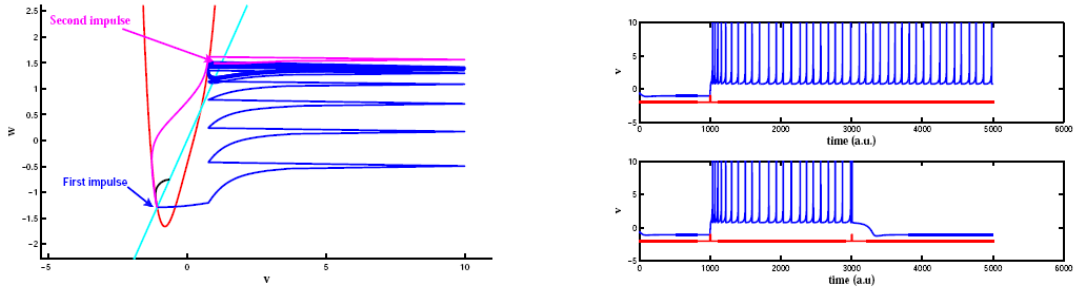

(a) Bistability: return to equilibrium via the same impulse

(b) Bistability

Figure 18: Bistability in the case of the quartic model

5.2 Bistability

Furthermore, we have seen that there exists cases where both the subthreshold dynamics and the adaptation sequence present stable orbits. These cases correspond to multistability: two different stable behaviors can appear depending on the initial condition, and perturbations can lead to switch from one behavior to the other (see figure 18.

5.3 Chaos

It is quite interesting to observe chaos in this model. Indeed, the firing patterns observed in the nervous system are often chaotic. For instance in the Purkinje cell, it has been observed that as the temperature increases for a given input current, the calcium spiking presented a period doubling during *in vitro* experiments (see [Mandelblat et al., 2001, Etzion and Grossman, 1998, Llinas and Sugimori, 1980, Hounsgaard and Midtgaard, 1989]). The appearance of doublets was also observed *in vivo* on recordings done by Jaeger and Bower on the ketamine-anesthetized guinea pig when the inhibition is blocked [Jaeger and Bower, 1994]. This type of route to chaos has also been shown in classical neuron models. For instance Rinzel and Miller in [Rinzel and Miller, 1980] located a period doubling on the interspike interval in the Hodgkin-Huxley model by computing eigenvalues along a family of periodic orbits. It has then been shown in other neuronal models, for instance in a version of the Hodgkin-Huxley model taking into account the temperature [Feudel et al., 2000]. In this case, the system undergoes a period doubling cascade when varying the temperature.

5.4 A good model of Purkinje cell

5.5 Electrophysiological classes

6 Conclusion

In this chapter we studied the spike patterns produced by neurons in the class of models introduced in [Touboul, 2008b]. We proved that the divergence of the nonlinearity F had to be fast enough for the model to be well defined. In this case, the study of a discrete map, the Poincaré application, lead us to distinguish between the different spike patterns fired, and the precise study of this map allows us to define electrophysiological classes depending on the parameters of the system having similar behaviors when varying the input current. We also proved that the system presented bifurcations in function of the reset value of the membrane potential, which can be related to in-vivo and in-vitro experiments.

A Cauchy Problem

The Cauchy problem consists in proving that there exists a unique solution to the problem (1.1) and (1.2) defined for all $t \in \mathbb{R}$ for a given initial condition (v_0, w_0) at time t_0. It was adressed by Romain Brette in [Brette, 2007] in the case of spiking models defined by a one dimensional ODE with a finite spiking threshold and a reset condition. He found that the reset introduced a countable and ordered set of backward solutions for a given initial condition, and this that this structure of solutions had important implications in terms of neural coding.

The case of the system given by (1.1) and (1.2) is slightly more complex, but can be treated in the same fashion as done in [Brette, 2007]. We have seen in section 2.7 that there exists a unique solution to the forward problem. Therefore in this appendix we are interested only in the backward solutions. The backward problem of equations (1.1) and (1.2) with initial conditions (v_0, w_0) at time t_0 corresponds to the forward solutions $v_b(t) = v(t_0 - t)$ and $w_b(t) = w(t_0 - t)$. of the system:

$$\begin{cases} \frac{\mathrm{d}v_b}{\mathrm{d}t} = -F(v) + w - I \\ \frac{\mathrm{d}w_b}{\mathrm{d}t} = -a(bv - w) \\ v_b(0) = v_0 \\ w_b(0) = w_0 \end{cases} \tag{A.1}$$

The nullclines for this system are the same as the nullclines of the forward problem, but the direction of the vector field changes. A new issue appears here: the membrane potential can may to $-\infty$ in finite time. In this case, the solution is not admissible. In the case of the adaptive exponential model, the backward membrane potential and the backward adaptation value will never blow up in finite time. Therefore, this solution is always an admissible solution. But in the case of the quartic model for instance, the membrane potential will

always blow up in finite time when the backward solution do not cross the v-nullcline, and such solutions will exist, for instance in the case where there is no fixed point: in the proof of theorem 3.1, we show that there exist a spiking solution for which the backward solution tends to infinity. For initial conditions of the backward problem below this orbit, because of Gronwall's theorem, the membrane potential will tend to $-\infty$ in finite time.

- If the backward solution does not blow up in finite time and does not cross the line $\{v_b = v_r\}$, then the solution of the backward equation is unique, and there exists a unique solution of the problem which is defined on $\mathbb{R}$.
- If the backward membrane potential blows up at time t_1 and its orbit does not intersect the line $\{v_b = v_r\}$ there is no solution to the Cauchy problem for $t \leq t_1$.
- If the backward orbit intersects the line $\{v_b = v_r\}$ then the problem splits in two solutions, one of which corresponding to a reset, and the other corresponding to the solution of the system (A.1). The branch of solution corresponding to a regular subthreshold backward problem is treated as described above. For the solution corresponding to a reset, we check if the value of the membrane potential at this point is inside the image of the Poincaré application. If it is the case, the admissible solutions correspond to the different reciprocal images of this value under Φ. There can exist two possible values: one that is inferior or equal to w^* and another one greater than w^*, and these two possible points are on the same orbit (the orbit starting above w^* crosses the line $v = v_r$ at the point below w^*). To avoid the difficulty or resetting at an infinite value of the membrane potential, we directly jump to the reciprocal image of this point by Φ, and compute the same way the possible branches of backward solutions.

Interestingly, in the case of the exponential model, since the backward solutions do not blow up in finite time, the backward solution is always an admissible solution. Therefore, we have a countable number of backward solution in this case.

In the case of the quartic model, the number admissible solutions is smaller. Indeed, the reciprocal images of Φ decrease, and when they are below the spiking trajectory diverging when $v \to -\infty$, the backward equation blows up in finite time. Therefore the only admissible solution is a spiking solution. Figure 19 illustrates the construction of a backward solution and of the Cauchy problem. From a given initial condition (v_0, w_0), if the backward solution never crosses the reset line $\{v = v_r\}$ there is only one admissible solution provided it does not blow up in finite time. If the backward solution crosses the reset line (star (1) and (2) of figure 19), the solution splits into two solutions, one of which corresponds to a spike when it exists (star (1)) and the other one corresponding to the regular solution of the backward equation (for star (2) no spiking solution correspond to the related adaptation value). Below the bold line corresponding to a diverging solution of the backward equation, in the case of models such as the quartic one, the only admissible solution is a spiking solution (star (3)).

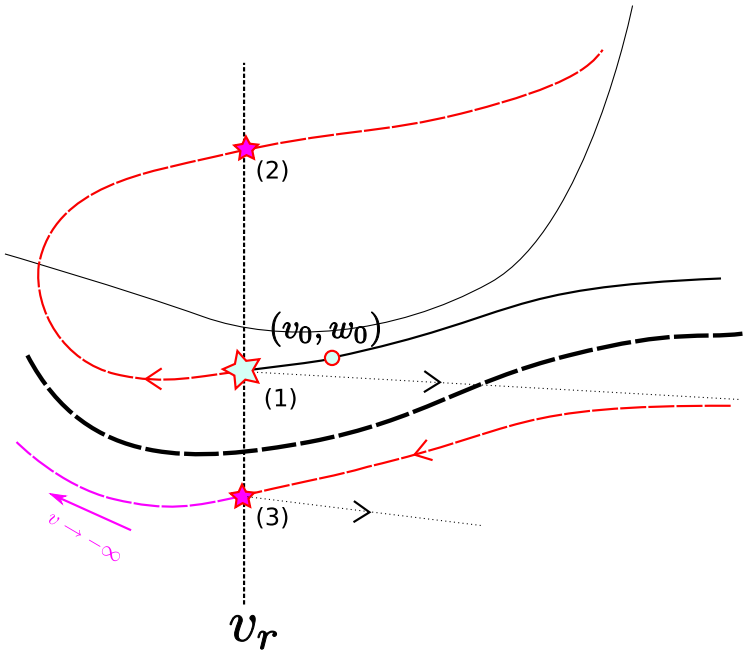

Figure 19: Construction of the backward set of solutions. Description in the text.

B Oscillations

To understand whether the stable manifold can cross the w-nullcline and possibly the V-nullcline, we study the asymptotic behavior of the solutions when $t \to -\infty$. The idea is the following: if the manifold goes to $-\infty$ (for V), then the derivative of the nonlinear term vanishes tends to its limit $F'_{-\infty}$ which can either be finite, or $-\infty$. In the following we shall assume that the manifold does not cross the V-nullcline. In that case, the voltage $V(t)$ of the manifold, seen as a solution of the system, goes to $-\infty$ as $t \to -\infty$, and we will look for possible contradictions.

If we have $F'_{-\infty} = -\infty$, the trajectories are asymptotically horizontal and hence will necessarily cross the w-nullcline, but not necesarily the v-nullcline. In the case where $F'_{-\infty} > -\infty$, the approximated dynamics can be solved analytically. Asymptotically, the differential equations satisfied by a given solution (v, w) of the rescaled model can be approximated by:

$$\begin{cases} \dot{v} &= F'_{-\infty} v - w + I \\ \dot{w} &= a(b\, v - w) \end{cases} \tag{B.1}$$

When $t \to -\infty$, the solutions of the linear system either spiral around the fixed point (complex eigenvalues) or align asymptotically to the direction of eigenvector associated to the smallest negative eigenvalue of the matrix L governing the dynamics of the linear system (B.1):

$$L = \begin{pmatrix} F'_{-\infty} & -1 \\ ab & -a \end{pmatrix}$$

If the eigenvalues of this matrix are complex, i.e., when $b > \frac{(a+F'_{-\infty})^2}{4a}$, then the solutions spiral around the fixed point. Therefore the trajectories cross the V-nullcline, which contradicts our initial hypothesis. Thus when $b > \frac{(a+F'_{-\infty})^2}{4a}$ (resonator regime), the stable manifold crosses both nullclines.

If the eigenvalues are real, the trajectories of the linear system align asymptotically to the direction of the lower eigenvalue

$$\lambda_- = -\frac{1}{2}(a - F'_{-\infty} + \sqrt{(F'_{-\infty} + a)^2 - 4a\, b})$$

This eigenvalue is always strictly negative hence solutions will diverge when $t \to -\infty$. The eigenvector associated with this eigenvalue is:

$$\begin{pmatrix} \frac{2}{a+F'_{-\infty}+\sqrt{(F'_{-\infty}+a)^2-4a\, b}} \\ 1 \end{pmatrix}$$

The slope of that eigenvector is always inferior to $F'_{-\infty}$, so that (linearized) trajectories do not cross the V-nullcline. However they can cross the w-nullcline when the slope of the eigenvector is smaller than b, i.e.:

$$\frac{a + F'_{-\infty} + \sqrt{(F'_{-\infty} + a)^2 - 4a\,b}}{2} < b$$

and this condition is satisfied when $b > \frac{1}{2}(a + F'_{-\infty})$. Assuming $\bar{a} > 0$, the inequality is always true if $\bar{\tau_w} > -F'_{-\infty}$; when when $\bar{\tau_w} < -F'_{-\infty}$, the inequality is never true given that the eigenvalues are real ($b > \frac{(a+F'_{-\infty})^2}{4a}$).

In summary, the stable manifold crosses both nullclines when $b > \frac{1}{2}(a + F'_{-\infty})$(resonator regime), and it crosses at least the w-nullcline when $\bar{\tau_w} > -F'_{-\infty}$ or $F'_{-\infty} = -\infty$.

References

[Brette, 2007] Brette, R. (2007). The cauchy problem for one-dimensional spiking neuron models. *Cognitive Neurodynamics*, 2(1):21–27.

[Brette and Gerstner, 2005] Brette, R. and Gerstner, W. (2005). Adaptive exponential integrate-and-fire model as an effective description of neuronal activity. *Journal of Neurophysiology*, 94:3637–3642.

[Clopath et al., 2007] Clopath, C., Jolivet, R., Rauch, A., Lüscher, H., and Gerstner, W. (2007). Predicting neuronal activity with simple models of the threshold type: Adaptive Exponential Integrate-and-Fire model with two compartments. *Neurocomputing*, 70(10-12):1668–1673.

[Devaney, 2003] Devaney, R. (2003). *An Introduction to Chaotic Dynamical Systems*. Westview Press.

[Dieudonné, 1963] Dieudonné, J. (1963). *Éléments d'analyse - Tome I : Fondements de l'analyse moderne*. Gauthier-Villars.

[Etzion and Grossman, 1998] Etzion, Y. and Grossman, Y. (1998). Potassium currents modulation of calcium spike firing in dendrites of cerebellar Purkinje cells. *Experimental Brain Research*, 122(3):283–294.

[Feudel et al., 2000] Feudel, U., Neiman, A., Pei, X., Wojtenek, W., Braun, H., Huber, M., and Moss, F. (2000). Homoclinic bifurcation in a Hodgkin–Huxley model of thermally sensitive neurons. *Chaos: An Interdisciplinary Journal of Nonlinear Science*, 10:231.

[Fourcaud-Trocme et al., 2003] Fourcaud-Trocme, N., Hansel, D., van Vreeswijk, C., and Brunel, N. (2003). How Spike Generation Mechanisms Determine the Neuronal Response to Fluctuating Inputs. *Journal of Neuroscience*, 23(37):11628.

[Gronwall, 1919] Gronwall, T. H. (1919). Note on the derivative with respect to a parameter of the solutions of a system of differential equations. *Annals of Mathematics*, 20:292–296.

[Hounsgaard and Midtgaard, 1989] Hounsgaard, J. and Midtgaard, J. (1989). Synaptic control of excitability in turtle cerebellar Purkinje cells. *The Journal of Physiology*, 409:157.

[Izhikevich, 2003] Izhikevich, E. (2003). Simple model of spiking neurons. *IEEE Transactions on Neural Networks*, 14(6):1569–1572.

[Izhikevich, 2004] Izhikevich, E. (2004). Which model to use for cortical spiking neurons? *IEEE Trans Neural Netw*, 15(5):1063–1070.

[Izhikevich, 2007] Izhikevich, E. (2007). *Dynamical Systems in Neuroscience: The Geometry of Excitability And Bursting*. MIT Press.

[Izhikevich, 2006] Izhikevich, E. M. (2006). *Dynamical Systems in Neuroscience: The Geometry of Excitability and Bursting*. The MIT Press. To appear.

[Izhikevich and Edelman, 2008] Izhikevich, E. M. and Edelman, G. M. (2008). Large-scale model of mammalian thalamocortical systems. *Proc Natl Acad Sci U S A*, 105(9):3593–3598.

[Jaeger and Bower, 1994] Jaeger, D. and Bower, J. (1994). Prolonged responses in rat cerebellar Purkinje cells following activation of the granule cell layer: an intracellular in vitro and in vivo investigation. *Experimental Brain Research*, 100(2):200–214.

[Jolivet et al., 2008] Jolivet, R., Kobayashi, R., Rauch, A., Naud, R., Shinomoto, S., and Gerstner, W. (2008). A benchmark test for a quantitative assessment of simple neuron models. *Journal of Neuroscience Methods*, 169(2):417–424.

[Koch and Segev, 1998] Koch, C. and Segev, I., editors (1998). *Methods in Neuronal Modeling: From Ions to Networks*. The MIT Press.

[Kuznetsov, 1998] Kuznetsov, Y. A. (1998). *Elements of Applied Bifurcation Theory*. Applied Mathematical Sciences. Springer, 2nd edition.

[Li and Yorke, 1975] Li, T. and Yorke, J. (1975). Period three implies chaos. *American Mathematical Monthly*, 82:985–992.

[Llinas and Sugimori, 1980] Llinas, R. and Sugimori, M. (1980). Electrophysiological properties of in vitro Purkinje cell somata in mammalian cerebellar slices. *The Journal of Physiology*, 305(1):171–195.

[Mandelblat et al., 2001] Mandelblat, Y., Etzion, Y., Grossman, Y., and Golomb, D. (2001). Period Doubling of Calcium Spike Firing in a Model of a Purkinje Cell Dendrite. *Journal of Computational Neuroscience*, 11(1):43–62.

[Rinzel and Ermentrout, 1989] Rinzel, J. and Ermentrout, B. (1989). *Analysis of neural excitability and oscillations*. MIT Press.

[Rinzel and Miller, 1980] Rinzel, J. and Miller, R. (1980). Numerical calculation of stable and unstable periodic solutions to the Hodgkin-Huxley equations. *Math. Biosci*, 49:27–59.

[Touboul, 2008a] Touboul, J. (2008a). Bifurcation analysis of a general class of non-linear integrate and fire neurons. 68(4):1045–1079.

[Touboul, 2008b] Touboul, J. (2008b). Bifurcation analysis of a general class of nonlinear integrate-and-fire neurons. *SIAM Journal on Applied Mathematics*, 68(4):1045–1079.

[Touboul, 2008c] Touboul, J. (2008c). Sensitivity to the cutoff value in the quadratic adaptive integrate-and-fire model. Research Report 6634, INRIA.

[Touboul and Brette, 2008] Touboul, J. and Brette, R. (2008). Dynamics and bifurcations of the adaptive exponential integrate-and-fire model. *Biological Cybernetics (submitted)*.

Unité de recherche INRIA Sophia Antipolis
2004, route des Lucioles - BP 93 - 06902 Sophia Antipolis Cedex (France)

Unité de recherche INRIA Futurs : Parc Club Orsay Université - ZAC des Vignes
4, rue Jacques Monod - 91893 ORSAY Cedex (France)
Unité de recherche INRIA Lorraine : LORIA, Technopôle de Nancy-Brabois - Campus scientifique
615, rue du Jardin Botanique - BP 101 - 54602 Villers-lès-Nancy Cedex (France)
Unité de recherche INRIA Rennes : IRISA, Campus universitaire de Beaulieu - 35042 Rennes Cedex (France)
Unité de recherche INRIA Rhône-Alpes : 655, avenue de l'Europe - 38334 Montbonnot Saint-Ismier (France)
Unité de recherche INRIA Rocquencourt : Domaine de Voluceau - Rocquencourt - BP 105 - 78153 Le Chesnay Cedex (France)

Éditeur
INRIA - Domaine de Voluceau - Rocquencourt, BP 105 - 78153 Le Chesnay Cedex (France)
http://www.inria.fr
ISSN 0249-6399